DEVELOPMENTAL BIOLOGY **181,** 121–143 (1997)
ARTICLE NO. DB968429

Soma–Germ Cell Interactions in *Caenorhabditis elegans:* Multiple Events of Hermaphrodite Germline Development Require the Somatic Sheath and Spermathecal Lineages

James McCarter, Bart Bartlett, Thanh Dang, and Tim Schedl[1]
Department of Genetics, Washington University School of Medicine, St. Louis, Missouri 63110

Germ cells complete multiple events to form functional oocytes and sperm. In the *Caenorhabditis elegans* hermaphrodite, germ cells develop in proximity to the somatic gonad sheath and spermathecal cells. We present evidence from cellular laser ablation studies indicating that cells of the somatic sheath and spermathecal lineages play critical roles in four events of hermaphrodite germline development. (1) Cells of the sheath and spermathecal lineage support germline proliferation; ablation of sheath/spermathecal precursor cells reduces mitotic proliferation. (2) These cells also play a role in the exit of germ cells from the pachytene stage of meiotic prophase and/or gamete differentiation; ablation can result in undifferentiated germ cells arrested in pachytene. (3) Proximal sheath and distal spermatheca cells are required for ovulation of the oocyte. During wild-type ovulation, the mature oocyte is expelled from the gonad arm by contraction of the proximal myoepithelial sheath and dilation of the distal spermatheca. Ablation of these cells traps mature oocytes in the gonad arm where they endomitotically replicate their DNA (the Emo phenotype). (4) Cells of the sheath and spermathecal lineage also appear to promote the male germ cell fate since ablation of one sheath/spermathecal precursor cell can feminize the hermaphrodite germ line. These somatic ablation-induced germline phenotypes demonstrate that the somatic gonad is required for multiple events in *C. elegans* germline development. Further, these results suggest that soma to germline cell–cell interactions in *C. elegans* are physiological in character (i.e., contraction during ovulation) as well as regulatory.

INTRODUCTION

Germline development in metazoans requires completion of multiple events to produce gametes. In the *Caenorhabditis elegans* hermaphrodite, for example, germ cells (1) proliferate mitotically, (2) specify their sexual identity, (3) enter the meiotic pathway, (4) progress through meiotic prophase, (5) differentiate as functional sperm or oocytes, (6) exit the gonad arm (e.g., ovulation of oocytes), and (7) complete fertilization in the spermatheca. In this paper, we demonstrate that many of these germline events in *C. elegans* depend upon signals or support from the surrounding somatic cells.

The somatic gonad has been shown to be important for germline development in a number of biological systems. In *Drosophila,* the dorsal/ventral and anterior/posterior patterning of both the oocyte and the surrounding somatic follicle cells is under genetic control which requires oocyte-to-soma and soma-to-oocyte communication (Ray and Schupbach, 1996; Bownes, 1994; St. Johnson, 1994). Initially, the oocyte signals to the follicle cells to specify dorsal and posterior fates, a process requiring the Gurken protein in the oocyte and the Torpedo protein in follicle cells (Schupbach, 1987; Neuman-Silberg and Schupbach, 1993; Roth *et al.,* 1995). The products of the Notch and Delta genes are involved in cell–cell signaling for anterior/posterior axis establishment (Ruohola *et al.,* 1991). After dorsal/ventral polarity is established in follicle cells, it is communicated back to the egg through a signaling cascade including Pipe, Nudel, and Windbeutel proteins produced by the soma and Easter, snake, Spätzle, and Toll proteins from the oocyte (Stein *et al.,* 1991; Chasan and Anderson, 1989;

[1] To whom correspondence should be addressed at Department of Genetics, Washington University School of Medicine, Box 8232, 4566 Scott Ave., St. Louis, MO 63110. Fax: 314-362-7855. E-mail: ts@genetics.wustl.edu.

0012-1606/97 $25.00

Anderson and Nusslein-Volhard, 1984). Mutations which disrupt the function of these genes during oogenesis result in maternal-effect embryonic lethality. Germline sex determination in *Drosophila* also requires somatic input. 2X:2A germ cells, which normally become oocytes, differentiate as spermatocytes when placed into a male soma (Steinmann-Zwicky *et al.*, 1989; Nothinger *et al.*, 1989). Genetic analysis has identified components of a putative soma to germ cell pathway for germline sex determination (Steinmann-Zwicky, 1992).

In mammals, germ cells depend on somatic cells during migration and proliferation. Sertoli and Granulosa cells release the ligand Steel which interacts with the Kit receptor tyrosine kinase on the surface of the germ cells (Fleischman, 1993). *In vitro* evidence suggests that the Steel/Kit pathway may permit survival of the germ cells rather than promote either migration or proliferation (Dolci *et al.*, 1991; Godin *et al.*, 1991). In the testis, the somatic Sertoli cells also inhibit the entry of germ cells into the meiotic pathway and induce the male fate (McLaren, 1991). In the mammalian ovary, follicle cells maintain oocyte cell cycle arrest in prophase of meiosis I by producing cAMP that is delivered to the oocyte via gap junctions (Buccione *et al.*, 1990; Wickramasinghe and Albertini, 1993). These findings in *Drosophila* and mammals reveal that germ cells derive specific information from interactions with somatic cells; multiple developmental events are regulated by ligand/receptor interactions or by diffusion of second messengers.

In addition to specific molecular signals, cell–cell interactions can include broader categories of dependence such as nutritional support, where one cell depends on another for importing nutrients, or structural/functional support, where one cell relies on another to maintain position or move. In mammals, for example, Sertoli cells import metabolites for germ cells through a blood–testis barrier and provide structural support for the testis in which the germ cells reside (Jegou, 1992). In the ovary, follicle cell metabolic activity directly effects the rate of oocyte growth (Buccione *et al.*, 1987). Ovarian smooth muscle contraction may play a role in expelling the oocyte from the ovary at ovulation (Diaz-Infante *et al.*, 1975).

The reproducible lineage and simple anatomy of the somatic gonad make *C. elegans* an excellent model organism for the identification of soma to germline cell–cell interactions. Laser ablation has been a particularly successful tool in uncovering these interactions. Ablation of somatic gonad cells allowed the discovery of the best characterized somatic gonad–germline interaction, the DTC–GLP-1 signaling pathway. In late larvae and adults, germ cells proliferate mitotically at the distal end of the gonad arm and enter meiotic prophase as they move proximally. Following ablation of the somatic distal tip cell (DTC) with a laser microbeam, the distal germline stem cell population is eliminated; all germ cells enter meiotic prophase (Kimble and White, 1981). This result indicated that germline proliferation depends on the DTC and in turn led to a search for mutations with a similar Glp (germline proliferation defective) phenotype (Austin and Kimble, 1987). Extensive genetic and molecular analysis resulted in the conclusion that a DTC-produced signal, encoded by the *lag-2* gene, interacts with a germline receptor, encoded by *glp-1*, to maintain a distal stem cell population. LAG-2 belongs to the Delta/Serrate/LAG-2 ligand family (Lambie and Kimble, 1991; Tax *et al.*, 1994; Henderson *et al.*, 1994), and GLP-1 is a member of the LIN-12/Notch/GLP-1 family of transmembrane receptors (Austin and Kimble, 1987, 1989; Priess *et al.*, 1987; Yochem and Greenwald, 1989). Another somatic ablation experiment had an opposing effect; eliminating most of the somatic precursor cells in the proximal hermaphrodite gonad causes mitotic proliferation in the proximal germ line, presumably due to ectopic stimulation of GLP-1 (Seydoux *et al.*, 1990). These ablation experiments established roles for the *C. elegans* somatic gonad in both direct induction of germ cell fate by a ligand/receptor interaction and in prevention of an inappropriate induction.

To uncover additional soma to germline cell–cell interactions in the *C. elegans* hermaphrodite, we performed laser ablation experiments concentrating on the somatic gonadal sheath and spermathecal lineages. Based on their position, cells from these somatic lineages are excellent candidates for interacting with the germ line; the sheath/spermathecal precursor cells are in close contact with germ cells during larval development, and the progeny sheath cells directly contact the germ line in the adult. The studies presented here demonstrate that removal of cells within the sheath and spermathecal lineages can result in four distinct germline defects resulting in sterility: (1) reduced germline proliferation, (2) defective exit of germ cells from the pachytene stage of meiotic prophase and/or defective gametogenesis, (3) failed ovulation of mature oocytes, and (4) feminization of the germ line. We demonstrate that oocytes depend on the sheath for myoepithelial contractions at ovulation for their exit from the gonad, a clear example of a structural/functional interaction as opposed to a regulatory interaction. We argue that somatic regulation of pachytene exit may occur by direct signaling, while the observed effect on proliferation may involve either signaling or nutritional support.

MATERIALS AND METHODS

Nematode Strains, Nomenclature, and General Methods

General methods for *C. elegans* culture and manipulation were as described (Brenner, 1974; Sulston and Hodgkin, 1988). Incubations were carried out at 20°C and observations were made at room temperature (20–23°C), unless otherwise noted.

The following *C. elegans* strains were used: N2 (wild-type reference strain, *Bristol*); LG (linkage group) I; *fog-1(q180)* (Barton and Kimble, 1990), *unc-13(e1091 and e51)*, *fog-3(q443)* (Ellis and Kimble, 1995), *unc-54(e190)* (Waterston *et al.*, 1980); LGII; *tra-2(e1095)* (Hodgkin and Brenner, 1977); LGIII; *ncl-1(e1865)* (Hedgecock and Herman, 1995), *unc-36(e251)*, *unc-32(e189)*, *glp-1(oz112gf)* (Berry *et al.*, 1997); LGIV; *fem-3(e1996)* (Hodgkin, 1986), *fem-3 (q20gf)* (Barton *et al.*, 1987), *let-60(n1046gf)* (Ferguson and Horvitz, 1985),

ced-3(n717) (Ellis and Horvitz, 1986); LGV; *fog-2(q71)* (Schedl and Kimble, 1988); LGX; and *ceh-18(mg57)* (Greenstein *et al.*, 1994).

Observations were also performed using the species *Caenorhabditis briggsae* (Fodor *et al.*, 1983).

Laser Ablations

Laser ablation has been used successfully in *C. elegans* as a tool to infer the developmental role of cells in embryos and larvae and the function of cells in the adult (Bargmann and Avery, 1995). Ablations of cells of the hermaphrodite gonad were performed using a nitrogen pulse laser (Laser Sciences Inc.) as described (Avery and Horvitz, 1987). The beam was directed through a Zeiss Axioplan microscope with the 100× objective, and laser intensity was adjusted by the use of neutral density filters. One hundred to 250 laser pulses were applied, until the cell's nucleolus had disappeared and its nuclear boundary was nondistinct. Worms were anesthetized with 10 m*M* Na azide in M9 and recovered within 25 min. Animals with evidence of collateral laser damage or mishandling, such as leakage through the gonadal basement membrane, or slow growth after recovery were discarded.

Somatic cells in the larval gonad were identified for ablation by their position and morphology (Kimble and Hirsh, 1979) using Nomarski differential interference microscopy. Frequent targets were the sheath/spermatheca precursor cells (SS cells) Z1.ap, Z1.paa, Z4.app, and Z4.pa (Figs. 1a and 1b). Ablations of SS cells were performed within a few hours before or after the L2/L3 molt. No significant differences in outcomes were seen with ablation time except those noted in the tables. Ablations were performed upon gonads in both the 5R and 5L orientations with the same outcomes. Additional ablations were performed at mid-L4 when germ cells are undifferentiated or a few primary spermatocytes are visible. Ablations were performed in the wild-type strain N2 unless otherwise noted. Additional strains used include *ncl-1(e1865), ncl-1(e1865) unc-36(e251),* and *fog-2(q71).* In a *ncl-1* background, nucleoli are enlarged in somatic cells, allowing these cells to be more easily differentiated from germ cells. No differences in outcomes were seen with different strains except those noted in the tables.

Killing of laser-targeted cell(s) was confirmed by counting the cell nuclei remaining in the ablated lineage in Nomarski-imaged young adults or in DAPI-stained dissected adult gonads. Nomarski imaging was particularly useful for counting spermathecal cells, whereas dissection followed by DAPI staining was used to count sheath cells, which cannot always be unambiguously distinguished from the surrounding germ cells by Nomarski in the adult. 2 SS cell ablation always refers to the ablation of both SS cells in the same arm. Ablation of 2 SS cells reduces the number of spermathecal cells in the arm from 24 to 6 and reduces the number of sheath cells in the arm from 10 to 0. 1 SS cell ablation reduces the number of spermathecal cells in the arm to 15 and the number of sheath cells in the arm to 5.

Synchronization of Populations for Ablation and Time Course

Populations were synchronized by ''lay-off'' and ''subsequent hatch-off.'' Fifty to 100 adults were transferred to a plate and allowed to lay eggs for 2 hr. Eleven to 14 hr after lay-off, threefold embryos were transferred to plates and allowed to hatch for 1 hr. Unhatched embryos were removed. These synchronized L1 populations reach the L2/L3 molt in 24 hr and mid-L4 in 48 hr at 20°C. Examination of cellular position and morphology in L2/L3 and L4 (Fig. 1) was used to precisely identify the proper stages for ablation.

Examination, Gonadal Dissection, and Cytology

Observations of living animals by Nomarski microscopy were as described (Sulston and Hodgkin, 1988) using a Zeiss Axioskop. Nematode gonads were dissected, fixed, and stained as described (Francis *et al.*, 1995). Briefly, worms in 1× PBS with 0.25 m*M* levamisole were decapitated with syringe needles, resulting in gonad extrusion. Extruded gonads were placed in fixative within 3 min. For epifluorescence visualization of DNA, dissected worms were fixed in cold methanol for 5 min, washed in PBS, and incubated in PBS with 100 n*M* DAPI for 15 min. For visualization of actin, dissected worms were fixed in formaldehyde for 2 hr, extracted in acetone for 3 min, washed in PBS, and incubated in PBS with 0.165 μM rhodamine–phalloidin (Molecular Probes) for 20 min (modified from Strome, 1986). For visualization of UNC-87 (Goetinck and Waterston, 1994), dissected worms were fixed in formaldehyde for 2 hr and cold methanol for 5 min, washed in PBS, and incubated in PBS with Tween, BSA, and a 1:5 dilution of affinity-purified UNC-87 antibody (a gift of S. Goetinck and R. Waterston). Gonads were transferred by capillary pipet to agarose pads on slides for viewing.

Time-Lapse Nomarski Microscopy

Worms were anesthetized for 45 min in a solution of M9 with 0.1% tricaine and 0.01% tetramisole (Sigma, Inc.) before viewing (protocol modified from Kirby *et al.*, 1990). Tricaine/tetramisole blocks body wall movement while still allowing oocyte maturation and ovulation. During anesthesia, pharyngeal pumping and egg laying cease. New oocytes are not formed at the loop of the gonad arm, presumably because nutrient availability from the intestine diminishes. Oocyte maturation, sheath and spermathecal activity at ovulation, and fertilization, however, all continue undisturbed for the first four to five oocytes in the arm. Worms can be rescued from an anesthetic exposure of up to 4 hr.

Animals were mounted on 3% agarose pads with 5 μl of the anesthetic and covered with an 18-mm square glass coverslip. The edges of the agarose were trimmed. The coverslip and slide were covered with a 30-mm square piece of plastic wrap to seal in moisture. A hole in the wrap accommodates the microscope objective. Animals were mounted on a Zeiss Axioskop and viewed with low light using the 40× or 63× lens. An infrared filter was added to the light path to prevent heating of the specimen. The microscope was connected to a Sony CCD video camera module XC-75 and Panasonic S-VHS VCR Model ag6720A. Time-lapse recordings were made at 1/12 real time. For each recording, the events of oocyte development, maturation, and ovulation were viewed. In animals in which cell ablations have been performed, or in mutant animals, any deviation from wild-type timing or morphology was noted. Sheath activity was quantitated by visually counting the number of contractions occurring in the myoepithelium over 3-min intervals. Contractions were counted twice and averaged.

RESULTS

Laser ablations of somatic gonad cells were initiated to investigate whether the elimination of specific somatic cells could generate reproducible defects in germline devel-

opment. If the elimination of a somatic cell(s) disrupts an event in germline development, we can infer a function for that somatic cell(s) in supporting the germline event. A description of *C. elegans* germline and somatic gonad development and adult anatomy is presented first, along with a description of the cells targeted for ablation. We then describe the four germline phenotypes which result from somatic ablations and present further experiments undertaken to clarify the origin of each defect.

Development of the Hermaphrodite Germ Line and Somatic Gonad

At hatching, the *C. elegans* gonad primordium is composed of two germ cells, Z2 and Z3, flanked by two somatic cells, Z1 and Z4. Germ cell proliferation occurs throughout larval development (L1–L4) and into adulthood. During larval development, the gonad forms two reflexed tubular arms, each containing a syncytium of germline nuclei sharing a common cytoplasm. (By convention, each germline nucleus and its surrounding cytoplasm is called a germ cell.) By L4, germ cell mitotic proliferation is limited to the distal ends of the gonad. As germ cells move proximally, they exit the mitotic cycle, enter the meiotic pathway, and progress through the stages of meiotic prophase I. Gametes differentiate in the proximal gonad; a brief period of sperm production in late L4 is followed by continuous oocyte production in the adult (Hirsh *et al.*, 1976; Kimble and Ward, 1988; Clifford *et al.*, 1994).

The nearly invariant lineage leading to all 143 somatic gonad cells has been characterized (Kimble and Hirsh, 1979), making possible the unambiguous identification of cells for ablation. During L1–L2, the lineages arising from Z1 and Z4 produce two DTC's, the anchor cell (AC), and nine somatic precursor cells. Initially, these 12 somatic cells partially surround the centrally located germ cells. In late L2, the nine somatic precursor cells and AC reorganize to form a central ''somatic primordium'' that segregates the germ cells into the anterior and posterior gonad arms (Fig. 1a). Migration of the DTC's, at either end of the gonad, results in elongation of the arms. Somatic divisions resume in L3 giving rise to the sheath, spermathecal, and uterine cells by mid-L4. In the adult gonad, the DTC and sheath directly contact the developing germ cells along the arm, while the spermatheca and uterus are located more proximally, away from the germ line. Two developmental stages used for ablation are now presented in detail.

(a) L2/L3 molt. The essentially invariant anatomy of the somatic primordium at the L2/L3 molt allows the rapid and reproducible identification of somatic precursor cells without cell lineaging. Ablations can therefore be performed in a relatively large number of animals. Somatic precursor cells take up similar, nearly symmetrical, positions in all animals (Fig. 1a), with the AC, DU cells (dorsal uterine precursor cells), and VU cells (ventral uterine precursor cells) located proximally and the SS cells (sheath/spermathecal precursor cells) located more distally (Kimble and Hirsh, 1979). The nuclei of the SS cells swell in late L2, making them distinct from the neighboring germ cells (Fig. 1b). Somatic precursor cells can be easily identified from several hours before the molt until several hours into L3, when somatic divisions resume. In animals where no ablation has been performed, each SS cell will go on to generate five sheath and nine spermathecal cells (Fig. 1c).

(b) Mid-L4. Mid-L4 marks the end of somatic divisions. After their birth, sheath cells migrate distally on the inside surface of the gonad basement membrane. Each arm contains 10 sheath cells (5 pairs), which connect proximally to the 24 spermathecal cells (18 SS cell-derived and 6 DU cell-derived), which in turn connect to the uterine cells via a junction of six nuclei (DU cell-derived and VU cell-derived) (Kimble and Hirsh, 1979) (Fig. 1d). The spermathecal cells form two groups: 8 distal cells aligned in two rows form a narrow corridor to the gonad arm, while 16 proximal cells form a wider bag-like chamber. The nuclei of the most proximal sheath cells, pairs 4 and 5, are located proximally and laterally to the neighboring germ cells. The nuclei of sheath pairs 2 and 3, in the process of distal migration at mid-L4, are located midway through the proximal arm. The nuclei of the first sheath pair are distal to the gonad loop and are larger than the nearby germ cell nuclei.

Structure of the Adult Sheath and Spermatheca

In the adult, the five sheath pairs form a thin (~0.4 μm) covering, encircling much of the gonad arm and the germ cells inside. The proximal three pairs form a nonstriated myoepithelium that contracts during ovulation to expel the oocyte from the gonad arm (Ward and Carrel, 1979). The myoepithelium contains several known muscle components. Electron micrographs of the sheath show interdigitated thick and thin filaments (Hirsh *et al.*, 1976; Strome, 1986). Staining of the sheath with anti-actin and anti-myosin antibodies or rhodamine–phalloidin (R-ph), which detects actin, reveals a filamentous network (Strome, 1986). An antibody to UNC-87, a *C. elegans* thin-filament-associated muscle protein (Goetinck and Waterston, 1994), also recognizes sheath filaments (data not shown), and punctate fluorescence is observed in the sheath *in vivo* with an α-integrin::GFP construct (B. Williams, personal communication).

We have inferred the location of boundaries between the proximal sheath cells from the R-ph staining pattern. Networks of actin fibers in each cell are separated from those of neighboring cells by narrow (1.0–2.5 μm) borders that lack staining (Figs. 2a and 2b). The borders may represent space between sheath cells or space between filaments and the edges of the cells. From the position of the borders in R-ph-stained gonads, we have constructed the three-dimensional arrangement of the proximal sheath cells; the cells intercalate with one another as interlocking diamonds, covering the surface of the gonad tube (Fig. 2c). The same borders are also observed in gonads *in vivo* with α-integrin::GFP (B. Williams, personal communication) and in fixed gonads stained with anti-UNC-87 antibody (data not shown).

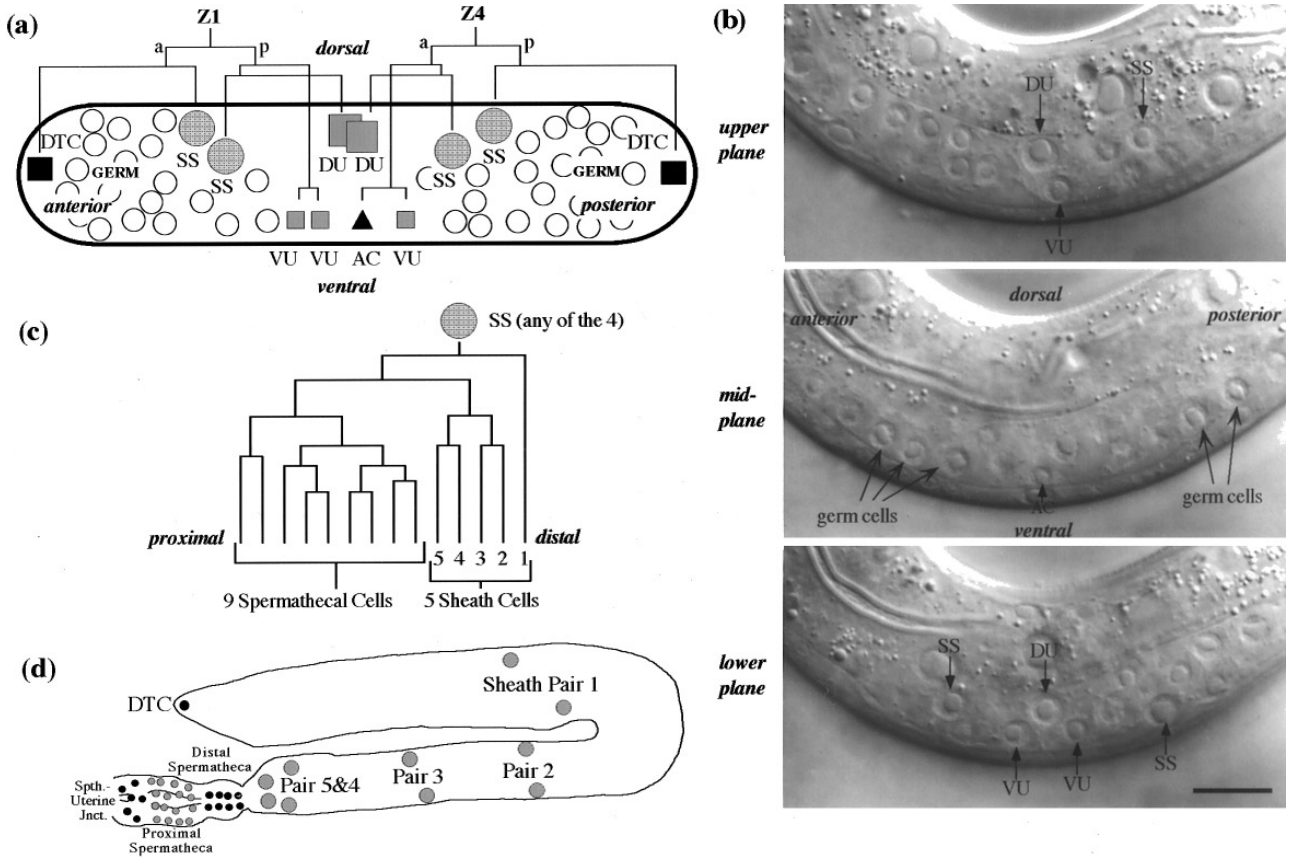

FIG. 1. Hermaphrodite gonad at the L2/L3 molt and at mid-L4. (a) A schematic of the gonad somatic primordium after L2 reorganization (5L configuration). The lineage giving rise to each somatic cell from Z1 and Z4 is shown. Germ cell nuclei are depicted as unfilled circles and somatic nuclei as filled shapes: DTC, distal tip cell (black square); SS cell, sheath/spermathecal precursor cell (gray circles); AC, anchor cell (black triangle); VU cell, ventral uterine precursor cell (small gray square); DU cell, dorsal uterine precursor cell (large gray square). The centrally located somatic primordium includes all of the somatic cells except the DTCs and is nearly symmetric around the AC. (b) Micrographs of the gonad at the L2/L3 molt (Nomarski optics). The somatic primordium of one hermaphrodite is shown in three focal planes (5L configuration). Nuclei appear as recessed shadows surrounding a protruding nucleolus. SS precursor cell nuclei lie at the anterior and posterior edges of the primordium in the upper and lower focal planes (right and left of the animal, respectively) and are noticeably larger than the germ nuclei next to them. (Z1.paa, Z4.app, and Z4.pa are visible. Z1.ap is above the focal planes presented.) Bar, 10 μm. (c) The lineage arising from each sheath/spermatheca (SS) precursor cell generates 9 spermathecal and 5 sheath cells. 2 SS cells contribute to each arm. (d) A schematic of the mid-L4 gonad arm noting the positions of somatic nuclei. All 10 sheath cells and 18 of the spermathecal cells arise from the SS cell lineages. Six of the proximal spermathecal cells are generated by the DU cells. The 6 cells of the spermatheca–uterine junction are generated by the DU and VU cells. (Lineages adapted from Kimble and Hirsh, 1979.)

Thin filaments are first detected in the sheath by R-ph at mid-L4, following the appearance of primary spermatocytes in the germ line. Initially, a small number of faintly staining fibers are seen in the proximal three sheath pairs. Fibers encircle the nucleus, and large gaps remain between the fibers in each cell and those of its neighbors, suggesting that either the cells do not yet fully cover the proximal gonad surface or that the myofilament lattice does not yet fill the cells. By the young adult stage, sheath fibers are more densely arrayed and strongly staining, and only a narrow border separates the group of fibers in one cell from those in a neighboring cell.

In the adult, sheath cells vary in their filament distribution by distal to proximal position. The first sheath cell pair (most distal) contains few filaments; a faint band of circumferential fibers, visible by R-ph and anti-UNC-87, wraps around the gonad distal to the loop (data not shown). The distal boundary of the first sheath pair is undefined by fluorescence microscopy, but cross-sectional electron micrographs reveal that the cells terminate midway through the distal gonad without contacting the DTC (J. White and E. Southgate, personal communication). A portion of the distal germ line, therefore, lacks contact with somatic cells and is covered only by basement membrane. The second sheath cell pair, which spans the gonad loop, also contains few filaments; short woolly fibers without a preferential

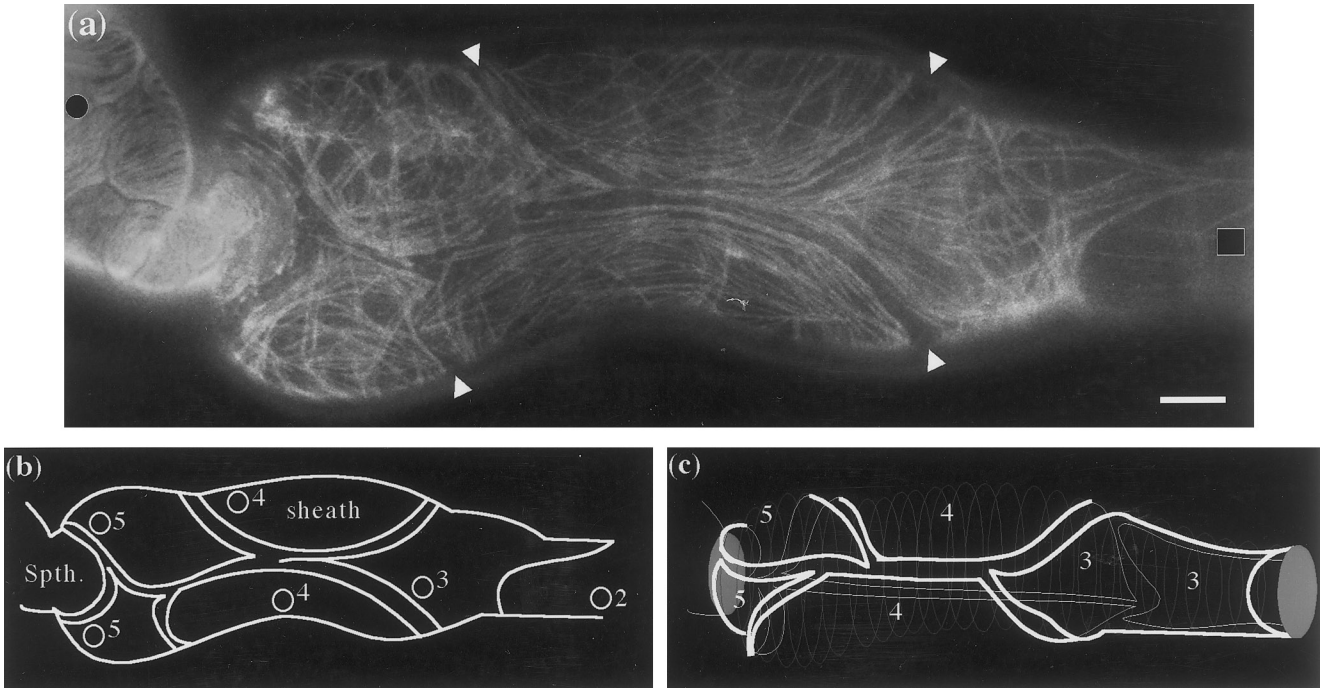

FIG. 2. Myoepithelial structure and cellular arrangement of the adult hermaphrodite proximal gonad sheath. (a) Rhodamine–phalloidin fluorescence from a dissected gonad arm shows a network of actin microfilaments in the proximal sheath (center) and spermatheca (left) (described by Strome, 1986). The narrow neck of the distal spermatheca and wider pouch-like arrangement of the proximal spermatheca are visible. Triangles indicate nonstaining regions that are likely boundaries between sheath cells. Square, distal. Circle, proximal. Bar, 10 μm. (b) A schematic of the proximal sheath boundaries based on (a). Nuclear positions (filled circles) are known from DAPI costaining (not shown). Numbers label sheath cells. (c) A three-dimensional schematic of the interlocking sheath cells based on (a) and additional stained gonad arms (n = 14) examined in multiple focal planes. White lines indicate sheath cell outlines (thick lines, foreground; thin lines, background). Gray rings depict the shape of the gonad tube.

direction are sometimes seen. The third sheath pair has a large number of longitudinally oriented filaments which increase in density toward the proximal end (Fig. 2a). The fourth sheath cell pair contains a dense array of longitudinal filaments, while in the fifth pair, both longitudinal and circumferential fibers are prominent. Longitudinal fibers in these cells likely generate contractile force along the distal–proximal axis of the gonad (i.e., pull rather than pinch).

Spermathecal cells contain actin; however, myosin has not been detected. Spaces in the actin network between spermathecal cells reveal the position of individual cells (Fig. 2a; Strome, 1986). Like the sheath cells, spermathecal cells intercalate closely with each other, but unlike the sheath, their microfilaments are predominantly circumferential (Fig. 2a), suited to the role of circumferential dilation during ovulation rather than longitudinal contraction. The eight distal spermathecal cells form a narrow corridor (2 rows of cells) that appears to act as a gate separating oocytes in the gonad arm from sperm in the pouch-like proximal spermatheca where fertilization occurs.

Oocyte Maturation and Ovulation

Oocyte maturation and ovulation in *C. elegans* can be observed by time-lapse Nomarksi microscopy (Ward and Carrel, 1979; Materials and Methods). Oocytes complete development in the proximal gonad arm while in diakinesis of meiotic prophase I (Figs. 3a and 4a). Meiotic maturation, the cell cycle transition from meiotic prophase to metaphase, occurs in the most proximal oocyte; the nuclear envelope breaks down and the oocyte becomes spherical. Ovulation, which moves the oocyte into the spermatheca, follows maturation by several minutes; contractions of the sheath increase in rate and intensity and pull the dilating distal spermatheca over the first oocyte. Fertilization occurs as the oocyte enters the spermatheca.

Effects of Cell Ablations on Somatic Gonad Structure

Sheath cells migrate distally inside the basement membrane of the gonad arm, which is probably laid down by the DTC and germ cells. Laser ablation of the sheath/spermatheca precursor (SS) cells at the L2/L3 molt, or ablation of combinations of sheath cells at mid-L4, does not affect the integrity of the basement membrane; leakage from the gonad is not seen ($n > 100$). In fact, an intact gonad is usually formed following L2/L3 ablation of the entire somatic primordium; in 5 of 6 cases, the anterior and posterior arms

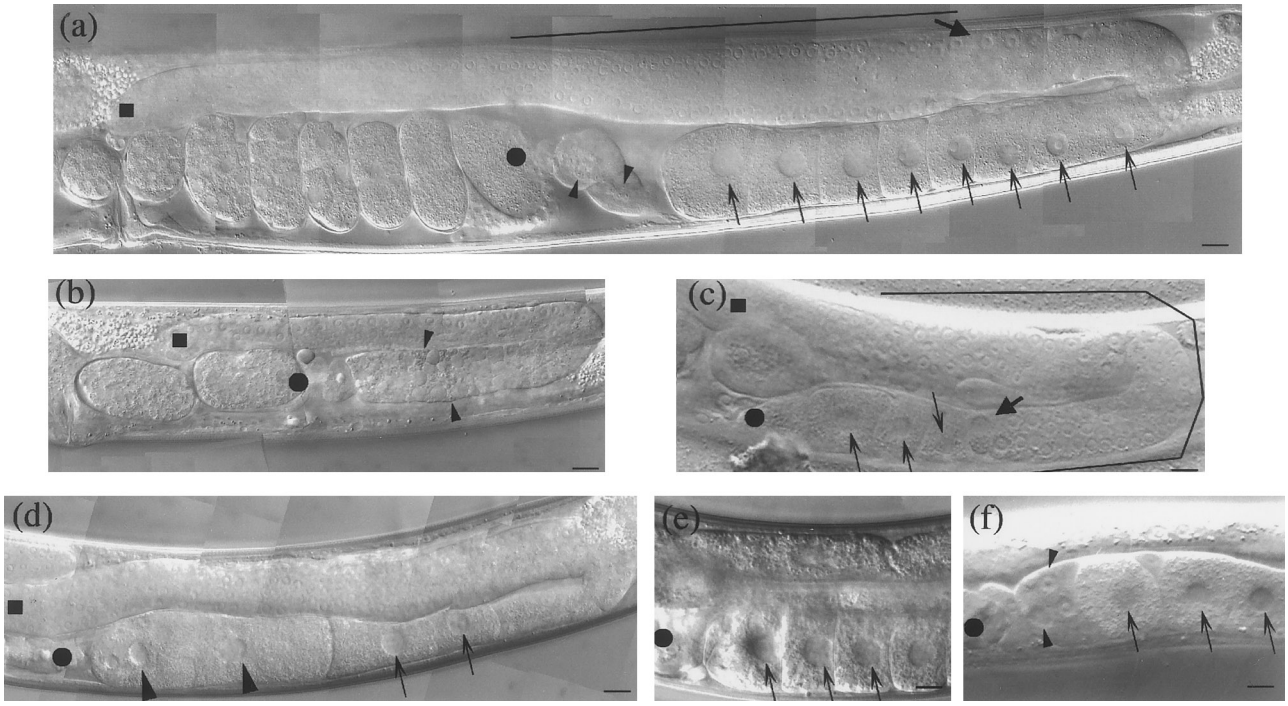

FIG. 3. Micrographs of wild-type and somatic cell-ablated adult hermaphrodite gonad arms, Nomarski optics (lateral view). (a) N2 wild-type adult gonad arm, internal view. Line along distal arm indicates region of the germline anuclear core. The thick arrow indicates the approximate position where germ cell volume begins to increase; moving proximally from this position, spacing between nuclei increases and the anuclear core is replaced by forming oocytes. Thin arrows indicate nuclei in diakinesis stage oocytes of the proximal arm with nuclear envelopes intact. Arrowheads indicate sperm in the spermatheca. Embryos are visible in the uterus. (b) Adult gonad arm defective in germline proliferation and pachytene exit following 2 SS cell ablation at the L2/L3 molt. The gonad is approximately one-fifth wild-type size with a reduced number of sperm in the arm (arrowheads) and no oocytes. The two embryos visible in the uterus were produced by the control arm (not shown) in which no ablations were performed. (c) Adult gonad arm with proximal restriction of the region of oogenesis following ablation of the distal sheath pair at mid-L4 (surface view). The thick arrow indicates the approximate position where the anuclear core is replaced by forming oocytes in the proximal arm. Thin arrows indicate oocyte nuclei. In a lower focal plane (not shown) the core extends around the loop and into the proximal arm (indicated by the line). In this surface view, the core is surrounded by small surface nuclei. (d) Adult gonad arm with the Emo phenotype following 1 SS cell ablation. Arrowheads indicate endomitotic nuclei. Thin arrows indicate nuclei of diakinesis stage oocytes. (e) Adult gonad arm with the Fog (feminization of the germ line) phenotype following 1 SS cell ablation. No sperm are present. Thin arrows indicate nuclei of diakinesis stage oocytes. Oocytes are compressed because larger numbers of oocytes are retained in the gonad arms of females (Doniach and Hodgkin, 1984; Kimble *et al.*, 1984). (f) Adult gonad with the Fog phenotype and proximal germ cells which appear undifferentiated (arrowheads) following 1 SS cell ablation. No sperm are present. Thin arrows indicate nuclei of diakinesis stage oocytes. Square, distal. Circle, proximal. Bar, 10 μm.

remained connected to one another into adulthood. When both SS cells or a single SS cell is ablated, the progeny cells are always missing, indicating that no alterations occur in other lineages to replace the missing cells. Gonad arms where both SS cells have been eliminated lack all sheath cells (by DAPI) ($n = 31$) and do not produce a myoepithelium (by R-ph) ($n = 2$). Other somatic gonad ablations can result in compensatory lineage alterations (Kimble, 1981; Seydoux *et al.*, 1990; Newman *et al.*, 1995). While replacement cells are not generated following 1 SS cell ablation, the remaining sheath cells do expand their usual territory so that the surface of the proximal gonadal tube is fully covered (Table 1). In 9 of 11 cases, no prominent gaps in the microfilament network existed, as assayed by R-ph staining. No gaps appeared following ablation of sheath cells in mid-L4 animals; the remaining cells covered the territory of their missing neighbors (Table 1). However, full sheath coverage of the gonad does not necessarily indicate that the myoepithelium can function properly in ovulation (see below).

Effects of Cell Ablations on Germline Development

2 SS Cell Ablation at the L2/L3 Molt: Defective Germline Proliferation (Glp)

Ablation of both sheath/spermathecal precursor (SS) cells in a gonad arm at the L2/L3 molt (2 SS cell ablation) eliminates the entire sheath as well as 18 spermathecal cells from the arm (Figs. 1a and 1c). This operation results in a

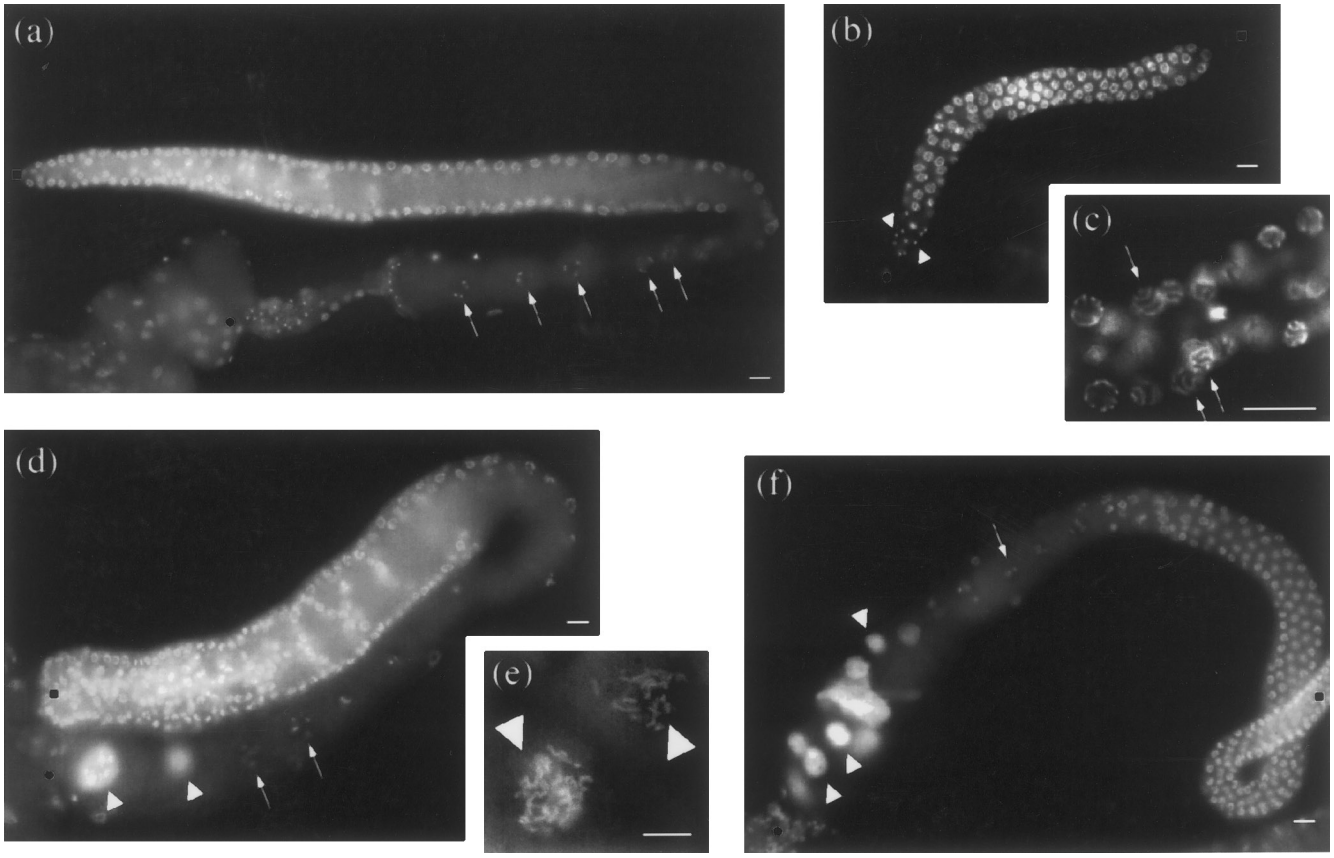

FIG. 4. Micrographs of dissected wild-type, somatic cell ablated, and mutant gonads stained with DAPI to visualize DNA. (a) N2 wild-type hermaphrodite adult gonad arm (internal view). Arrows indicate condensed bivalent chromosomes in diakinesis stage oocytes of the proximal arm. Sperm are visible in the proximal gonad arm and spermatheca. (b) Hermaphrodite adult gonad arm defective in germline proliferation and pachytene exit following 2 SS cell ablation at the L2/L3 molt. Arrowheads indicate sperm. (c) Enlargement of the proximal gonad arm in an adult hermaphrodite following 2 SS cell ablation. Arrows indicate germ nuclei in pachytene. (d) Hermaphrodite adult gonad with the endomitotic oocytes in the gonad arm (Emo) phenotype following 1 SS cell ablation (internal view). Arrowheads indicate endomitotic polyploid nuclei proximally. Arrows indicate chromosomes in diakinesis stage oocytes distal to the endomitotic nuclei. (e) Enlargement of the proximal gonad arm in an adult hermaphrodite following 1 SS cell ablation. Arrowheads indicate two polyploid oocyte nuclei with many condensed chromosomes. (f) *fog-1(q180)* adult male gonad arm with endomitotic oocytes (arrowheads). Arrow indicates chromosomes in a diakinesis stage oocyte distally. Square, distal. Circle, proximal. Bar, 10 μm.

sterile gonad arm defective in germline proliferation (Glp phenotype). 2 SS cell ablated gonad arms are small relative to control arms in which no ablation has been performed (compare Fig. 3a to 3b and Fig. 4a to 4b). The Glp phenotype is fully penetrant following 2 SS cell ablation (Table 2). By adulthood, the total number of germ cells produced per arm is approximately one-fifth of wild type (Table 3A), and the arms are about one-third wild-type length (~170 μm vs ~550 μm). Another phenotype observed in these arms, defective exit from pachytene, is discussed in the next section.

Defective germline proliferation is not seen in the arm following control ablations of the somatic DU cells, SS cells contributing to the opposite arm, or the AC (Table 7A). Ablation of 1 SS cell in the arm may decrease germ cell number slightly, but this has not been quantitated. L2/L3 ablation of all 10 cells of the somatic primordium results in a similar decrease in germline proliferation as is seen following 2 SS cell ablation (Table 3A), indicating that the Glp phenotype observed following the elimination of the 2 SS cells alone is not enhanced by the loss of the rest of the somatic cells. The Glp phenotype observed following somatic ablation is not a result of peripheral laser damage to germ cells; ablation of 2–4 germ cells in an arm at L2/L3 does not noticeably decrease germ cell number in the adult. Ablation of a large number of germ cells (i.e., 5 to 10 out of 17) does reduce germ cell number (Table 7B), but not as drastically as is seen following the 2 SS cell ablation.

The reduced germline proliferation phenotype observed following 2 SS cell ablation suggests that the SS cells or their descendants promote germline proliferation. DTC–GLP-1 signaling is a major pathway for promoting proliferation in the *C. elegans* germline. Disruption of DTC–GLP-1 signal-

TABLE 1

Sheath Coverage of the Gonad Arm Following SS Cell Lineage Ablation

Cell(s) ablated[a]	Stage ablated	% Arms with full sheath coverage[b]	*n*
None	—	100	20
1 SS cell	L2/L3 molt	81	11
2 proximal sheath cells	Mid-L4	100	6

[a] Ablation of 1 SS cell (sheath/spermathecal precursor) results in the absence of five sheath cells in the arm. Proximal sheath cells ablated in L4 were both #5's ($n = 2$), both #4's ($n = 3$), or one #3 and one #4 ($n = 1$). All cell ablations were verified (see Materials and Methods).

[b] Adult gonads were dissected and stained with R-ph for actin and DAPI for DNA. A gonad arm was scored as exhibiting full sheath coverage if actin fully covered the proximal gonad arm without gaps. The regions where the cells were ablated appear to have been covered by the remaining cells because myofilament coverage extended from the region of the intact cell into the region of the ablated cell without the spaces between cells like those seen in the unablated gonad (Fig. 2a).

ing by ablation of the DTC or in the *glp-1 loss-of-function (lf)* mutants results in elimination of the proliferative stem cell population as all germ cells enter meiotic prophase and differentiate as gametes (Kimble and White, 1981; Austin and Kimble, 1987). Strong *glp-1(lf)* mutations result in a sterile gonad arm with 5–20 germ cells. Two lines of evidence indicate that the SS cells promote germline proliferation in a manner independent of the DTC–GLP-1 signaling pathway. First, several findings suggest that a stem cell population is maintained following 2 SS ablation, unlike when DTC–GLP-1 signaling is disrupted. These observations include (a) germ cell numbers increase from the time of ablation (17–27 per arm) to adulthood (average of 257 per arm) and continue to increase through adulthood (Tables 3A and 3B); (b) mitotic figures are observed in the distal region by DAPI staining (data not shown); and (c) following 2 SS cell ablation, arms establish a distal-to-proximal polarity with cells entering meiotic pachytene proximally but not distally. Thus, the Glp phenotype observed following 2 SS cell ablation is distinct from the Glp phenotype observed following DTC ablation and in *glp-1(lf)* mutants.

Second, we performed a direct test of whether the SS cell effect on germline proliferation was GLP-1 dependent or independent. 2 SS cell ablations were performed in *glp-1(oz112gf)*, a gain-of-function (gf) mutant where germ cells proliferate independent of the DTC or GLP-1 ligand LAG-2 (Tax *et al.*, 1994; Henderson *et al.*, 1994), resulting in the formation of a germline tumor (Berry *et al.*, 1997). A reduction of proliferation in *glp-1(oz112gf)* following 2 SS cell ablation would suggest that these cells support germline proliferation by a GLP-1-independent mechanism. Alternatively, an identical level of proliferation in *glp-1(oz112gf)* with or without the SS cell lineage would suggest that these cells support proliferation via GLP-1 signaling. *unc-32(e189) glp-1(oz112gf)* hermaphrodites were raised at 25°C and 2 SS cell ablations were performed at the L2/L3 molt. Animals were fixed as L4's (35 hr posthatch) or as young adults (41 hr posthatch), and germ cells were counted in both the arm where the 2 SS cell ablation was performed and the control arm where no ablation was performed. Proliferation continued throughout the germ line in *glp-1(oz112gf)* following 2 SS cell ablation and no meiotic germ cells were observed, but the extent of proliferation was reduced substantially. At L4, the control arm where no cells had been ablated had 609 ± 292 germ cells, whereas the 2 SS cell ablated arm had only 248 ± 44 ($n = 3$). In young adults, the control arm had 1391 ± 491 germ cells, whereas the 2 SS cell ablated arm had 705 ± 231 germ cells ($n = 4$). This reduction in tumor germ cell number by half following 2 SS cell ablation suggests that the SS lineage cells support germline mitotic proliferation by a mechanism independent of GLP-1 signaling.

Cell death could provide an alternative explanation for the diminished size of the germ line following 2 SS cell ablation. However, no obvious signs of necrotic or programmed death were observed. To directly test whether programmed cell death plays a role, 2 SS cell ablations were performed in *ced-3(n717)* (Ellis and Horvitz, 1986) to see if this mutation could suppress the Glp phenotype. *ced-3(n717)* is known to block programmed cell death in the germ line (M. Hengartner, personal communication). Suppression was not observed; 100% of the arms were Glp ($n = 12$). This suggests that programmed cell death does not account for the diminished germ cell number following 2 SS cell ablation.

In summary, our observations of 2 SS cell ablated gonad arms indicate that cells of the SS lineage promote germline proliferation, although the mechanism of this support is unknown. This is the first evidence that somatic cells other than the DTC's are necessary to promote germline proliferation in *C. elegans*.

TABLE 2

Germline Proliferation (Glp) and Pachytene Exit Defects Resulting from Ablation of Two Sheath/Spermathecal Precursor Cells at the L2/L3 Molt

SS cells ablated[a]	% Glp and pachytene exit defective	*n*
None	0	50
Z1.ap and Z1.paa	100	26
Z4.pa and Z4.app	100	23

[a] 2 SS cells were ablated in either the anterior or posterior gonad arm. Ablations were verified in 31/49 arms. For the remaining 18 arms, failed dissection prevented verification of the absence of all SS cell progeny. The hermaphrodite DTC leader function in 2 SS cell ablated arms is apparently normal since DTC migration to form U-shaped gonad arms was observed in all cases.

TABLE 3

Quantitation of Germline Proliferation (Glp) and Pachytene Exit Defects Resulting from Ablation of Two Sheath/Spermathecal Precursor Cells at the L2/L3 Molt

Cells ablated	Time assayed, hr posthatch[a]	Number of germ cells in arm[b]	n
A. Germline proliferation defect			
None	48–60	1001 ± 141	3
2 SS cells	48–60	190 ± 15	5
None	60–90	1380 ± 177	3
2 SS cells	60–90	253 ± 94	8
Somatic primordium[c]	60–90	316 ± 84	9
None	135	1564 ± 75	3
2 SS cells	135	435 ± 10	2

Cells ablated	Ablations performed in	% of arms containing sperm	Number of sperm when present[d]	% of arms containing oocytes	Number of oocytes when present[d]	n
B. Pachytene exit defect						
None	Hermaphrodites	100	~160	100	>160	25
2 SS cells	Hermaphrodites	57	54 ± 44	4	1	23
Somatic primordium	Hermaphrodites	8	16	0	0	12
None	Females[e]	0	na[f]	100	>30	25
2 SS cells	Females	0	na	24	1.5 ± 0.6	17

[a] Equivalently aged animals with and without cellular ablation were fixed at the indicated times in adulthood. (The L4 to adult molt occurs at ~45 hr posthatch at 20°C).

[b] Germ cell number was obtained by counting germ cell nuclei stained with DAPI in either dissected gonads or whole-mount animals.

[c] Somatic primordium ablation eliminates 10 somatic precursor cells: Z1.ap (SS), Z1.paa (SS), Z1.pap (DU), Z1.ppa (VU), Z1.ppp (VU or AC), Z4.aaa (AC or VU), Z4.aap (VU), Z4.apa (DU), Z4.app (SS), and Z4.pa (SS). In addition to the Glp and pachytene exit defects, ablation of the somatic primoridum resulted in germ cells with abnormal nuclear morphologies, including large decondensed nuclei distally (5/12 arms) and small condensed clustered nuclei proximally (2/12 arms), which were not seen in wild-type or in the 2 SS ablated animals.

[d] Unmated wild-type hermaphrodites produce at least 160 oocytes and unmated females at least 30. Mating into either hermaphrodites or females causes several hundred more oocytes to be produced. The number of germ cells that have undergone exit from pachytene is equivalent to the number of oocytes produced plus one-quarter of the number of sperm produced (since each male germ cell generates four sperm, whereas each female germ cell generates a single oocyte).

[e] Females were *fog-2(q71).*

[f] Not applicable.

2 SS Ablation at the L2/L3 Molt: Defective Pachytene Exit

Following distal mitotic proliferation, *C. elegans* germ cells progress through several stages of meiotic prophase (i.e., leptotene, zygotene, pachytene, diplotene, and diakinesis). Overt gametogenesis follows exit from the pachytene stage. 2 SS cell ablation at L2/L3 in hermaphrodites, in addition to reducing mitotic proliferation, results in defective germ cell exit from pachytene and/or defective gametogenesis. The phenotype is fully penetrant (Table 2). In gonad arms where 2 SS cells have been ablated, nuclei accumulate in pachytene (Fig. 4c) and fewer gametes are produced. While this phenotype may be due to either defective pachytene exit or defective gametogenesis, for simplicity we will refer to it as a pachytene exit defect. Following 2 SS cell ablation, only 57% of arms made sperm and the number of sperm made in these animals was diminished (Table 3B, Fig. 4b). Oogenesis was rarely observed (4%). Since hermaphrodites complete spermatogenesis before switching to oogenesis, the germ line in the 2 SS cell ablated arms may never reach this switch. To address whether the arms were capable of making oocytes, ablations were performed in females. Following 2 SS cell ablation in *fog-2(q71),* oocytes were observed in only 24% of the animals, suggesting that oogenesis is even more severely curtailed than spermatogenesis (24% vs 57%). Ablation of the entire somatic primordium enhances the pachytene exit defect, nearly eliminating gametogenesis (Table 3B). Defective pachytene exit is not observed following control ablations of either germ cells or other cells of the somatic primordium (Table 7).

RAS and MAP kinase pathway genes in *C. elegans,* such as *let-60 ras* (Han and Sternberg, 1990; Beitel *et al.,* 1990), *mek-2* (Kornfeld *et al.,* 1995; Wu *et al.,* 1995), and *mpk-1/sur-1* (Lackner *et al.,* 1994; Wu and Han, 1994), appear to promote exit from pachytene and/or gametogenesis (Church *et al.,* 1995). Mutations in these genes show a phenotype of

germ cells arrested in pachytene similar to that seen following 2 SS cell ablation (although these mutants also show abnormal packing of nuclei on the surface of the gonadal tube not seen following 2 SS ablation). Based on mosaic analysis, *mpk-1* MAP kinase and likely the other genes in the cascade act in the germ line to promote exit from pachytene/gametogenesis (Church *et al.*, 1995). The upstream signal that activates this pathway is not known. Elimination of a signal for pachytene exit/gametogenesis produced by the surrounding sheath might account for the germ cell pachytene arrest observed following 2 SS cell ablation. *let-60(n1046gf)* is a gain-of-function mutation that in some cases can stimulate the MAP kinase pathway in the absence of an upstream signal (Lackner *et al.*, 1994; Wu and Han, 1994). While *let-60(n1046gf)* has no germline phenotype alone, we reasoned that it might ameliorate the 2 SS cell ablation phenotype. However, following 2 SS cell ablation at L2/L3 in *let-60(n1046gf)*, exit from pachytene/gametogenesis was still defective; of five arms, one showed no differentiation, three produced a limited number of sperm, and one produced limited sperm and one oocyte. Therefore, *let-60 gf* does not appear to overcome the effects of 2 SS cell ablation [however, also see Sundaram *et al.* (1996) for additional information on *let-60(n1046gf)*]. Despite this negative result, it remains plausible that the soma acts through the RAS and MAP kinase cascade to signal germline pachytene exit.

To define the specific somatic cells whose elimination results in reduced germ cell exit from pachytene, cellular ablations were performed in mid-L4 after the divisions giving rise to all of the somatic gonad cells were complete. In adult hermaphrodite gonads where no cells were ablated, female (i.e., oocyte) germline nuclei exit pachytene as they round the gonad loop. Pachytene-stage nuclei are located on the surface of the gonad tube and surround a syncytial anuclear core extending through the distal gonad to the loop (Fig. 3a) (Abi-Rached and Brun, 1975; Gibert *et al.*, 1984; White, 1988). As cells exit pachytene and begin oogenesis, cell size increases so that the core is eliminated. Age affects the position of female germ cell pachytene exit; in most young adults, the core ends just proximal to the loop, whereas at 1–2 days into adulthood, more oocytes have formed proximally and in most cases the core ends distal to the loop (Fig. 3a). In 7 of 10 arms in which the distal sheath cell pair (pair number one) was ablated (Fig. 1d), the anuclear core extended proximally through the loop and about halfway into the proximal gonad arm; oocyte production was limited to a restricted proximal zone (Fig. 3c). In 3 of these arms that were successfully dissected and DAPI stained, the pachytene zone was also observed to extend proximally with the anuclear core (data not shown). This proximal extension of the core and restriction of oogenesis were also observed in 4 of 6 arms following ablation of three of the distal four sheath cells. The core retains this proximal extension late in adulthood in gonads where distal sheath cells have been ablated and does not move distally as occurs in wild type. Sperm production is unaffected, and despite the spatial shift in meiotic prophase progression and oogenesis, viable embryos are produced from the ablated gonad arm. These mid-L4 distal sheath cell ablations suggest a role for the distal sheath cells in promoting pachytene exit or oogenesis. The difficulty of reproducibly identifying all the distal sheath cells in 1 arm by Nomarski has precluded extending these observations. A more thorough series of ablations performed in a strain where the sheath cells are more easily identified (e.g., GFP labeled) will be required to further characterize the effect of sheath cell ablation on germ cell pachytene exit and oogenesis.

1 SS Cell Ablation at the L2/L3 Molt: Endomitotic Oocytes in the Gonad Arm (Emo)

The effect of 2 SS cell ablation on germline proliferation and pachytene exit masks the effect that the elimination of these cells has on later events in germline development. Partial elimination of the sheath and spermatheca, which allows for proliferation and differentiation, reveals two additional phenotypes: endomitotic oocytes in the gonad arm (Emo) and feminization of the germ line (Fog). The Emo and Fog phenotypes, both incompletely penetrant, occur independently of one another (see note to Table 4) and are discussed separately.

Ablation of any 1 SS cell at the L2/L3 molt eliminates 5 of 10 sheath cells in the arm along with 9 spermathecal cells (Figs. 1a and 1c). This ablation results in an endomitotic oocyte in the gonad arm (Emo) phenotype. Emo gonads are sterile with distended polyploid nuclei in the oocytes of the proximal gonad arm (Figs. 3d and 4d). Oocytes mature and exit diakinesis of meiotic prophase without being properly ovulated or fertilized (see below). Oocytes reenter the mitotic cycle, but do so endomitotically, i.e., multiple rounds of DNA replication occur in the absence of cytokinesis and karyokinesis (Iwasaki *et al.*, 1996). The 1 SS cell ablation-induced Emo phenotype is incompletely penetrant (44%), and similar results are seen following ablation of any 1 of the 4 SS cells (Table 4). Endomitotic oocytes are not seen in an arm following ablations of the DU cells, the AC, SS cells which contribute to the opposite arm, or germ cells (Table 7).

Three observations reveal that the polyploid genome of the oocytes observed following 1 SS cell ablation arises by ongoing endomitotic cycling. First, by time-lapse video Nomarski microscopy, cycles of nuclear envelope breakdown and reformation are observed. Second, endomitotic oocytes can be observed with either an intact or absent nuclear envelope (Fig. 3d) and with either condensed or decondensed chromosomes (Figs. 4d and 4e). When chromosomes are condensed, a large number of chromosomes (>50) can be observed. Third, the proximal oocytes, which become endomitotic before more distal oocytes, show more intense DAPI staining, suggesting that additional rounds of DNA replication have occurred. The absence of karyokinesis and cytokinesis in endomitotic oocytes likely reflects the lack of mitotic centrioles in unfertilized oocytes (Albertson, 1984). We have not investigated whether the divisions of meiosis I and II precede endomitotic cycling.

TABLE 4

Endomitotic Oocyte (Emo) Phenotype Resulting from Ablation of One Sheath/Spermathecal Precursor Cell at the L2/L3 Molt

Ablation	% Arms Emo[a]	*n*
None	0	50
1 SS cell (summary)[b]	44	98
Breakdown by cell		
Z1.ap	33	18
Z1.paa	45	29
Z4.pa	55	29
Z4.app	36	22
Breakdown by temperature (°C)[c]		
15	32	25
20	43	127
25	55	20

Note. Since both the Emo phenotype (Table 4) and the Fog phenotype (Table 6) result from 1 SS ablation in N2 with incomplete penetrance, we examined whether the phenotypes occurred independently or dependently. The null hypothesis that the occurrence of the two phenotypes is independent is supported by the χ^2 test (Norman and Streiner, 1994), $\chi^2 = 0.32$ (data not shown). A χ^2 value of 3.84 is required to reject the null hypothesis for $P < 0.05$. Gonadal sheath and spermathecal cellular arrangement are conserved between *C. elegans* and the related hermaphrodite *Caenorhabditis briggsae,* suggesting that the function of these cells is conserved between the two species. The Emo phenotype is observed following 1 SS cell ablation in *C. briggsae,* indicating likely conservation of the phenomenon between species, although the penetrance is lower than in *C. elegans* (19%, $n = 26$, 20°C).

[a] The presence or absence of the Emo phenotype was scored in the arm in which the 1 SS cell ablation was performed. Arms were scored for the Emo phenotype by DAPI staining to observe polyploid nuclei in the oocytes. Hermaphrodites were scored ⩾60 hr after hatch at 20°C. The onset of the Emo phenotype occurs prior to 60 hr posthatch in hermaphrodites. No increase in Emo penetrance occurs after 60 hr. Ablations performed at 15 and 25°C were also scored well into adulthood. The onset of the Emo phenotype is delayed in females (see Results).

[b] Ablations were performed in N2 at 20°C. Ablations were verified in 39 of 98 arms. (51% of the ablation-verified animals were endomitotic.) Failed dissections prevented verification in other arms.

[c] Ablations at various temperatures were performed in N2, *ncl-1(e1865),* and *ncl-1(e1865) unc-36(e251).* The penetrance of the Emo phenotype appears to increase with temperature.

Sheath and Spermatheca Cell Ablations in L4: Endomitotic Oocytes in the Gonad Arm (Emo)

To define the specific somatic cells whose elimination results in the Emo phenotype, ablations were performed in mid-L4 (Table 5, Fig. 1d). Ablation of the distal sheath pair alone did not result in endomitotic oocytes, whereas ablation of groups of proximal sheath cells did cause the Emo phenotype. Strikingly, ablation of the fourth and fifth sheath pairs together resulted in endomitosis with 95% penetrance. Ablation of the distal spermathecal cells also resulted in the Emo phenotype, whereas ablation of cells in the proximal spermatheca or spermathecal–uterine valve had no effect. These results demonstrate that (1) the cells needed to prevent Emo sterility are the proximal myoepithelial sheath and the distal spermathecal cells (which form the narrow corridor linking the gonad arm to the spermatheca), and (2) these cells are needed in late L4 or in the adult. While the sheath cells remaining after L2/L3 or L4 ablation expand their territories so that gaps are not usually observed in sheath coverage (Table 1), the Emo phenotype suggests that full coverage does not ensure normal function.

The Endomitotic Oocytes (Emo) Phenotype Occurs Following Defective Ovulation

To observe how endomitotic oocytes arise in the gonad arm after somatic cell ablation, time-lapse video Nomarski microscopy was performed. Following L2/L3 ablation of 1 SS cell, L4 ablation of sheath pairs 4 and 5, or L4 ablation of the distal 8 spermathecal cells, recordings were made in young adults during oocyte development, maturation, and ovulation of the first oocyte in the arm. Time-lapse microscopy indicates that following these ablations, animals are defective in ovulation and that oocytes become endomitotic in the gonad arm after maturing and failing to be ovulated properly.

In one 1 SS cell ablated animal, the oocyte developed and matured normally but failed to exit the gonad arm at ovulation; endomitotic cycling was then observed in the oocyte. In another 1 SS cell ablated animal, the mature oocyte partially entered the spermatheca, was fertilized, then ''fell-back'' into the gonad arm and began embryogenesis. Sheath contractions were observed in these gonads but appeared insufficient to fully pull the distal spermatheca over the oocyte. Following ablation of sheath pairs 4 and 5, oocytes matured in the gonad arm and ovulation did not occur ($n = 3$). The oocytes then began endomitotic cycling. Sheath activity was reduced from an average of 9.3 contractions per minute in wild-type to 3.7 contractions per minute in the proximal sheath ablated animals (rates based on counting 176 and 70 3-min intervals, respectively). In two animals in which the distal spermatheca was ablated, the mature oocyte began ovulation and was torn into two pieces as it entered the spermatheca; one piece fell-back into the gonad arm where it became endomitotic, while the other went on to form a miniature embryo in the uterus. Tearing of oocytes does not occur in wild type, presumably because the distal spermatheca fully closes behind the oocyte and prevents it from refluxing into the gonad arm as ovulation ends.

Intrigued by the observation of oocytes tearing during defective ovulation, we performed additional sheath and spermathecal ablations and examined young adults which had just begun maturation/ovulation. In addition to endomitotic oocytes in the gonad arm, we found miniature round embryos in the uterus, small endomitotic oocytes in the uterus, and small oocyte fragments in the proximal gonad arm without nuclear material. All of these defects can

TABLE 5

Endomitotic Oocyte (Emo) Phenotype Resulting from Ablation of Sheath and Spermathecal Cells at L4

Cells ablated[a]									
Sheath cell pairs[c]					Spermathecal cells[d]				
1st	2nd	3rd	4th	5th	Distal	Prox	Valve	% Arms Emo[b]	*n*
X								0	5
	X	X						0	1
		X	X					0	1
			X					0	2
	X	X	X	X				100	4
			X	X				95	22
				X				50	2
					X			50	6
						X		0	4
							X	0	4
No cells ablated								0	50

[a] Each row of the table represents a series of ablations. Ablated cells are indicated with an X and the outcome is indicated at the right. Ablations were verified in adults by DAPI staining to confirm that the nuclei of ablated cells were missing. Usually, the nuclei of ablated cells were completely missing. Occasionally, small DAPI staining fragments of the ablated nuclei were visible. In no cases did a cell recover and maintain a normal nucleus into adulthood. Unablated sheath cells are capable of expanding their territories to cover regions of the gonad where the ablated cells would have been (see Table 1).

[b] Arms were scored for the Emo phenotype by DAPI staining to observe polyploid nuclei in the oocytes. Animals were scored 60 hr or more after hatching.

[c] For sheath cell ablations, an X represents ablation of both cells in the pair.

[d] For spermatheca ablations, ''distal'' indicates ablation of six to eight cells of the distal spermatheca, ''prox'' indicates ablation of seven to eight cells of the proximal spermatheca, and''valve'' indicates ablation of four to six nuclei of the spermathecal–uterine valve (Fig. 1d).

be explained by the tearing of oocytes during defective ovulation.

In somatically ablated animals, the usual events of oocyte development (i.e., increasing cell volume, increasing nuclear volume, disappearance of the nucleolus, and distal migration of the nucleus) and oocyte maturation (i.e., nuclear envelope breakdown and cortical rearrangement) occurred in the correct temporal order. Endomitosis was never observed to occur in oocytes until after maturation and attempted ovulation. This supports the contention that the defect leading to endomitosis in the gonad arm is defective ovulation rather than a defect in meiotic cell cycle regulation or some other cause. The one effect we did see on oocyte maturation occurred following ablation of sheath pairs 4 and 5; this ablation frequently delayed the onset of maturation relative to control arms where no ablation was performed ($n = 14$, data not shown). This may indicate a role for the proximal sheath in promoting maturation, but further studies will be needed to substantiate this possibility.

A further observation also supports a defect in ovulation as the cause of the trapped Emo oocytes in the gonad arm following 1 SS cell ablation. *C. elegans* virgin females, such as *fog-2(q71)* (Schedl and Kimble, 1988), lack sperm and maintain their oocytes in diakinesis for extended periods of time before sporadic triggering of maturation and ovulation. We have found that the time when the first ovulation has occurred in 50% of the animals in a synchronized population is ~3 hr later in *fog-2(q71)* females than N2 hermaphrodites (data not shown). If the Emo phenotype following somatic ablation arises from defective ovulation, females should show a delay in the time of onset of the Emo phenotype. A delay would not necessarily be expected if the Emo phenotype arises from a meiotic cell cycle defect (Iwasaki *et al.*, 1996).

A delay in the onset of endomitosis is observed following 1 SS cell ablation in females. 1 SS cell ablations at the L2/L3 molt were performed in hermaphrodites and females [*fog-2(q71)*], and the animals scored for endomitosis when the first oocyte was ready for ovulation (50–55 hr posthatch). Whereas 55% of the hermaphrodite gonad arms were endomitotic ($n = 20$), only 7% of the female gonad arms were endomitotic ($n = 29$). Later (60–147 hr posthatch), after sporadic ovulation would have occurred in females, 1 SS cell ablated females and hermaphrodites show similar penetrance of the Emo phenotype [42% ($n = 24$) and 51% ($n = 93$), respectively]. By the χ^2 test (Norman and Streiner, 1994), the difference observed in the Emo penetrance in females and hermaphrodites at 50–55 hr posthatch was highly significant, ($\chi^2 = 14.1$, corresponding to $P < 0.001$). Further, we followed the status of several individual female gonad arms following 1 SS cell ablation; arms that were not Emo as young adults became Emo several hours later ($n = 4$). Additionally, 1 SS cell ablated females with arms that were not yet Emo were induced to ovulate by the introduction of sperm through mating. Following mating, all became

TABLE 6

Feminization of the Germline (Fog) Phenotype Resulting from Ablation of One Sheath/Spermathecal Precursor Cell at the L2/L3 Molt

Ablation[a]	% Arm fully Fog[b]	% Arm partial Fog[c]	% Undiff cells[d]	*n*
None	0	0	0	50
1 SS cell (summary)	44	9	9	141
Breakdown by cell				
Z1.ap	47	9	9	32
Z1.paa	49	5	16	37
Z4.pa	44	5	2	41
Z4.app	35	19	10	31

Note. Ablations performed at 15 and 25°C also feminized, but with lower penetrance. At 15°C, 19% of arms were fully feminized ($n = 16$). At 25°C, 10% of arms were fully feminized ($n = 10$). The finding of germline feminization following 1 SS cell ablation is not an artifact of the N2 hermaphrodite stock used; a survey of our strain showed 0% feminization at 20°C when no ablation was performed ($n = 400$). Strangely, *ncl-1(el865)* appears to suppress feminization following 1 SS ablation; we observed only 2% full feminization and 4% partial feminization in this background ($n = 55$). *ncl-1* plays no known role in sex determination. The Fog phenotype was not observed following 1 SS cell ablation in *C. briggsae* ($n = 21$).

[a] 1 SS cell ablation was performed in the N2 wild-type strain at 20°C and verified in 53 of 141 arms. 55% of the ablation-verified arms were fully feminized and 15% were partially feminized. Failed dissections prevented verification in other arms.

[b] Arms were scored for lack of sperm in young adults by Nomarski and many confirmed in DAPI-stained dissected gonads.

[c] Arms considered partial Fog had fewer than eight visible sperm.

[d] Undifferentiated cells are defined here as cells lacking both sperm and oocyte characteristics found proximal to the oocytes. The undifferentiated germ cell phenotype is distinct from the pachytene arrest/gametogenesis defective phenotype observed following 2 SS cell ablation. In 1 SS cell ablated feminized gonads the undifferentiated germ cells are found proximal to the oocytes, while in the 2 SS cell ablated gonads, pachytene arrested germ cells are found distal to sperm when spermatogenesis is observed.

endomitotic ($n = 4$). These findings in females support the conclusion that mature oocytes become endomitotic after defective ovulation traps them in the gonad arm.

1 SS Cell Ablation at the L2/L3 Molt: Feminization of the Germ Line (Fog)

Each gonad arm of the wild-type *C. elegans* hermaphrodite produces ~160 sperm from ~40 primary spermatocytes before beginning oogenesis. Ablation of 1 SS cell in an arm at the L2/L3 molt leads to feminization of the germ line so that oocytes are produced without sperm (Table 6, Fig. 3e). The phenotype is indistinguishable from the *fem* and *fog* mutants (Nelson *et al.*, 1978; Kimble *et al.*, 1984; Doniach and Hodgkin, 1984; Hodgkin, 1986; Schedl and Kimble, 1988; Barton and Kimble, 1990; Ellis and Kimble, 1995), but occurs with incomplete penetrance (44%). 1 SS cell ablation can also result in partial feminization, where arms have a reduced number of sperm (9%). Some of the feminized arms also contain cells proximal to the oocytes that appear undifferentiated (9%) (Fig. 3f). These cells do not have characteristics of either male or female differentiated germ cells and are similar to the proximal undifferentiated cells occasionally seen in certain feminizing mutant backgrounds, such as *fem-3(e1996)*/+ females (our observations) and in temperature-pulsed *fem-2(b245)* males (L. Edgar and D. Hirsh, personal communication); it is possible that these cells have a confused gender identity.

Feminization following somatic gonad cell ablation suggests a potential role for the somatic gonad in influencing germline sex determination. If the somatic gonad acted near the end of the genetic pathway for germline sex determination (Clifford *et al.*, 1994), 1 SS cell ablation might suppress the masculinization of the germline (Mog) phenotype seen in *fem-3(q20gf)* at 25°C (Barton *et al.*, 1987). No such suppression was observed; all arms remained fully Mog following 1 SS cell ablation ($n = 22$), suggesting that if the somatic gonad ablation acts through the defined sex determination pathway, it has its effect upstream of *fem-3*.

Ablation of other somatic gonad primordium cells can also result in the Fog phenotype at very low penetrance; 11% feminization of the arms is observed following ablation of both dorsal uterine precursor cells (Table 7A). It might be predicted that ablation of larger numbers of somatic primordium cells would increase feminization, but this was not observed. Following 2 SS cell ablation, male germline development still occurs (sperm were produced 57% of the time; Table 3B). Even when the entire somatic primordium was eliminated, 1 of 12 arms still produced some sperm. However, it is not known at what point(s) in the gonadal lineage the somatic cells influence the germ line to promote male development. Possibly, somatic gonad cell ablations at an earlier time would lead to complete feminization.

The germline feminization phenotype differs from the other phenotypes induced by ablation of somatic gonad cells in that feminization can also be induced by direct ablation of germ cells. We found that germ cell ablation at the L2/L3 molt results in low penetrance feminization (Table 7B); ablation of 2–4 germ cells yielded 13% feminization ($n = 40$), while ablation of 5–10 germ cells caused 38% feminization ($n = 8$). Feminization was observed following ablation of germ cells located proximally (15%, $n = 41$) or distally (29%, $n = 7$) in the gonad arm. We considered that the somatic gonad cell ablation-induced Fog phenotype might stem from peripheral damage to the germ cells. However, if this were the case we would expect higher penetrance feminization to result from direct targeting of germ cells, and this was not observed. It therefore seems likely that somatic ablation-induced and germline ablation-induced feminization are separate phenomena. We can postulate no direct mechanism for how germ cell ablation results in feminization. Feminization of the germ line has been induced by treatment with light-activated psoralen in L1 and early

TABLE 7
Control Ablations of Somatic and Germ Cells at the L2/L3 Molt

Cell(s) ablated	% Glp	% Pachytene exit defective	% Emo	% Fog	*n*[a]
		A. Somatic cell ablations Arm opposite to ablation scored[b]			
SS cell ablations					
Z1.ap or Z1.paa	0	0	0	0	8
Z1.ap and Z1.paa	0	0	0	0	9 (2)
Z4.pa or Z4.app	0	0	0	0	5 (3)
Z4.pa and Z4.app	0	0	0	0	2 (1)
DU cell ablations		Both arms scored[c]			
Z1.pap	0	0	0	7	24 (14)
Z4.apa	0	0	0	0	28 (10)
Z1.pap and Z4.apa	0	0	0	11	18
Cells ablated	% Glp[e]	% Pachytene exit defective	% Emo	% Fog	*n*
		B. Germ cell ablations Ablated arm score			
2–4 cells/arm	0	0	0	13	40
5–10 cells/arm	50	0	0	38	8

[a] The sample size used to determine the percentage incidence of the Glp, pachytene exit, and Emo phenotypes is listed first. The sample size used to determine the percentage incidence of the Fog phenotype is listed in parentheses. Only cell ablations performed in N2 were scored for the Fog phenotype.

[b] SS cells were ablated in one arm, and the opposite arm was scored for the four phenotypes in the adult. Somatic cells were all present in the arm where no cells were ablated.

[c] The dorsal uterine (DU) cells are located in the center of the somatic primordium. Since each DU precursor cell contributes cells to a common uterus and to the proximal portion of both the anterior and posterior spermatheca, both arms were scored. Percentage incidence of each phenotype is calculated per gonad arm. Following anchor cell ablation (Z1.ppp or Z4.aaa), none of the four phenotypes were observed ($n = 5$).

[d] Germ cells were ablated in an arm at the L2/L3 molt and the same arm was scored for phenotypes in the adult. Similar results were seen whether ablations were performed in late L2 or early L3. In late L2, there are 18 ± 4 germ cells present per arm, $n = 11$, range 13–24. In early L3, there are 27 ± 4 germ cells per arm, $n = 11$, range 21–32. Germ cell ablations were performed exclusively in N2.

[e] The germline proliferation (Glp) defect observed following ablation of 5–10 germ cells per arm is not as pronounced as that seen following 2 SS ablation. Medium-sized arms are observed in the adult with fewer germ cells than are seen in wild type ($\sim\frac{1}{2}$ size). Arms that produce sperm and oocytes are fertile.

L2 (Edgar and Hirsh, 1985), but the mechanism of this effect remains equally obscure.

Conceivably, the effect of somatic ablation on germline sex determination may be an indirect effect resulting from changing germline size and play no direct role in regulating sex determination. 2 SS cell ablation substantially reduces both gonadal volume and germ cell number, and 1 SS cell ablation may slightly reduce the size of the germ line. We also observe occasional feminization of the germ line following direct ablation of germ cells which reduces germline size. Changing the size of the germ line may alter the relative levels/activities of various sex determination proteins to one another. For instance, if levels of the products of the *fem* genes were reduced, but levels of *tra-2* gene product were maintained, the *fem* gene products might not be activated to promote sperm production.

Mutants with Somatic Gonad Abnormalities: Endomitotic Oocytes and Other Phenotypes

Since ablation of sheath and spermathecal cells, or their precursors, results in specific defects in germline development, we investigated mutations which affect specification, differentiation, or function of these cells to see if similar germline phenotypes were present. In various mutants, we observed the Emo phenotype along with evidence of defective ovulation, as well as defective germline proliferation and pachytene exit.

(a) unc-54. *unc-54* encodes myosin B, the major myosin heavy chain isoform of body wall muscle (MacLeod *et. al.*, 1977; Miller *et al.*, 1986). *unc-54* is expressed in the sheath along with *myo-3*, which encodes myosin A (Okkema *et al.*, 1993). Myosin is also detected by antibody staining in

TABLE 8
Germline Phenotypes in *unc-54 (e190)*

Phenotype	Penetrance (%)
Sterility[a]	14
Endomitotic oocytes in the arm (Emo)	13
Endomitotic oocytes in the uterus	3
Small fragments of oocytes in the arm	13
Small spherical embryos	2

Note. Phenotypes were determined by Nomarski microscopy (n = 150) using a population of animals raised at 20°C and examined in the first day of adulthood (older adults are egg-laying defective and therefore uninformative). The endomitotic oocytes in the gonad arm (Emo) phenotype were confirmed by DAPI staining of dissected gonads. The penetrance of each phenotype is calculated per gonad arm.

[a] Sterility indicates gonad arms that produced no embryos. Because some phenotypes do not result in sterility, and some gonads display multiple phenotypes, the percentages of the phenotypes listed below sterility do not sum to 14%.

the sheath but not the spermatheca (Strome, 1986). Animals homozygous for the *unc-54* null mutation *e190* are nearly paralyzed but are viable and fertile (Dibb *et al.*, 1985). While the small brood size of *unc-54(e190)* animals is partly attributable to their deficient movement and egg laying, we have found that it also results from defective ovulation. In early adulthood, *unc-54(e190)* animals exhibit sterility (14% of gonad arms). Among the phenotypes observed are endomitotic oocytes in the gonad arm (13%) and uterus (3%), torn oocytes in the arm (13%), and small spherical embryos in the uterus (2%) (Table 8). Ovulations observed by time-lapse Nomarski were abnormal. For example, one oocyte was torn during ovulation: a portion proceeded into the spermatheca, was fertilized, and underwent embryogenesis. The other portion remained in the proximal gonad until a subsequent ovulation forced it into the uterus. Sheath contractions do occur in *unc-54(e190)* and their rate does rise during ovulation (n = 4), although the effectiveness of the contractions appears substandard. Based on these observations, the absence of myosin B likely results in defective contractile function in the sheath, causing defective ovulation and leading to phenotypes such as endomitotic oocytes in the gonad arm (Emo).

(b) ceh-18. *ceh-18* encodes a POU-domain homeobox protein that is found in the sheath and DTC nuclei, but not the spermatheca (Greenstein *et al.*, 1994). In the *ceh-18* mutant *mg57*, sheath nuclei are occasionally small or missing, and endomitotic oocytes are observed in the gonad arm (Emo phenotype) along with small spherical shaped embryos in the uterus (Greenstein *et al.*, 1994). We examined *ceh-18(mg57)* (n = 210) for comparison to sheath and spermatheca ablated animals and found endomitotic oocytes (10%) and small fragments of oocytes (2%) in the gonad arm, as well as endomitotic oocytes (10%) and small spherical embryos (2%) in the uterus. Time-lapse Nomarski microscopy of ovulation in *ceh-18(mg57)* revealed that the small spherical embryos seen in the uterus and small fragments of oocytes seen in the gonad arm can result from tearing of the oocyte during ovulation (n = 2). The *ceh-18(mg57)* mutation therefore seems to interfere with sheath specification, differentiation, or function, resulting in defective ovulation. In addition to displaying ovulation-related defects like endomitosis, *ceh-18(mg57)* has other phenotypes similar to those seen following somatic cell ablation. A few *ceh-18(mg57)* gonads are defective in germline proliferation and pachytene exit like those following 2 SS cell ablation (6%). Many have somewhat reduced germline proliferation compared to wild type (41%). Others show a proximal shift in the pachytene zone as is observed following ablation of the distal sheath pair (18%).

(c) fog-1 and fog-3. Males with mutations in *fog-1* or *fog-3* have a female germ line (i.e., oocytes) in a somatically male gonad (Barton and Kimble, 1990; Ellis and Kimble, 1995) The somatic male gonad has neither a sheath, spermatheca, nor any myoepithelial structure around the proximal gonad arm (Klass *et al.*, 1976) as is present in the hermaphrodite (Hirsh *et al.*, 1976). In adult XO male *fog-1(q180)* and *unc-13(e51) fog-3(q443)* homozygotes, oocytes in the gonad exit diakinesis and become endomitotic. This fully penetrant Emo phenotype (Fig. 4f) resembles that seen following 1 SS cell ablation: polyploid nuclei are observed proximal with more distal oocytes still in diakinesis. Most likely, oocytes are leaving diakinesis at maturation, but lacking any apparatus for ovulation or fertilization, they cycle endomitotically in the gonad arm.

DISCUSSION

Developing *C. elegans* germ cells are located in close proximity to cells of the somatic gonad sheath and spermathecal lineages. We have eliminated sheath and spermathecal cells to examine the role these cells play in the development of the germ line. These cell ablations result in four specific sterile phenotypes: (1) defective germline proliferation, (2) defective exit of germ cells from meiotic pachytene, (3) endomitotic oocytes in the gonad arm, and (4) germline feminization. These results provide new insight into processes of germline development that were not previously known to be dependent on somatic cells. We propose that sheath and spermathecal lineage cells are necessary to (1) promote germline proliferation, (2) promote pachytene exit and/or gametogenesis, (3) release oocytes from the gonad at ovulation, and (4) promote the male fate during germline sex determination. The multiple roles of somatic gonad cells in germline development revealed by DTC ablation (Kimble and White, 1981), somatic precursor ablation in L1 (Seydoux *et al.*, 1990), and SS cell ablation (this paper) are summarized in Table 9. Notably, in the many ablations performed where oocytes are produced and fertilized, no role has been found for the *C. elegans* somatic gonad in patterning the oocyte for embryogenesis, as is the case in *Drosophila* (see Introduction).

The ablation-induced phenotypes described are specific

TABLE 9

Summary Table: The Effect of Somatic Gonad Cell Ablations on Germline Development[a]

Cell(s) ablated	Stage	Defect observed[b]	Inferred function	Reference
DTC	L1 to adult	Germline proliferation defective, all proliferating germ cells enter the meiotic pathway (Glp)	DTC signals germ cells via GLP-1 to promote proliferation or inhibit entry into meiotic prophase	Kimble and White (1981)
SS/DU cell and VU cells[c]	Late L1	Proximal proliferation (Pro)	Somatic precursor cells prevent inappropriate signaling from the AC to GLP-1 in the germ line	Seydoux *et al.* (1990)
2 SS cells	L2/L3	Decreased germline proliferation (Glp)	SS lineage cells may signal germ cells via a GLP-1-independent pathway to promote proliferation or provide nutritive support for proliferation	This paper
2 SS cells	L2/L3	Pachytene exit and/or gametogenesis defective	SS lineage cells may signal germ cells to exit from pachytene/complete gametogenesis or provide nutritive support for these processes	This paper
1 SS cell, or prox sheath/distal spermatheca cells	L2/L3 or L4	Endomitotic oocytes in the gonad arm (Emo)	Proximal sheath cell contraction and distal spermatheca dilation are necessary for ovulation of the oocyte	This paper
1 SS cell	L2/L3	Feminization of the germline (Fog)	SS lineage cells may promote the male germ cell fate in hermaphrodites	This paper

[a] See text for definition of ablated cells and related references.

[b] See text for detailed descriptions of the phenotypes for ablations performed in this paper.

[c] For proximal proliferation to be observed with full penetrance in a gonad in the 5L configuration, the ablation must include Z1.pa and Z4.ap (SS/DU precursors), Z1.pp (VU/VU precursor), and Z4.aap (VU precursor); Z4.aaa (the AC) must remain unablated (Seydoux *et al.*, 1990). In most cases, 1 SS cell (Z1.ap and Z4.pa) was left unablated, though proximal proliferation still occurs when these cells are ablated as well (see Fig. 7, Seydoux *et al.*, 1990). These ablations were performed in late L1 and early L2. We never observed proximal proliferation following 1 or 2 SS cell ablation alone in late L2 or early L3.

to elimination of sheath and spermatheca somatic lineages and are not due to peripheral laser damage to the germ line. With the exception of germline feminization, none of the phenotypes observed can be mimicked by direct ablation of germ cells. Further, a lineage mutant, *shv-1(oz128),* has been isolated which transforms certain sheath and spermatheca precursor cells (Z1.ap and Z4.pa) into ectopic distal tip cells (R. Francis, M. T. Le, and T. Schedl, unpublished results). *shv-1* gonad arms established by the extra DTCs lack all sheath and spermathecal structures; these arms are defective in germline proliferation and pachytene exit/gametogenesis, mimicking the 2 SS cell ablation. *shv-1* gonad arms established by the original DTCs lack the descendants of 1 SS cell and display both endomitotic oocytes in the gonad arm and feminization of the germ line, mimicking the 1 SS cell ablation. Therefore, whether gonad arms missing sheath and spermathecal cells are formed by genetic lineage transformation or laser ablation, essentially the same phenotypes are observed.

Many of the germline phenotypes we observed following somatic ablation occurred with incomplete penetrance or variable expressivity. For example, after 2 SS cell ablation, 43% of arms were completely defective in pachytene exit and gametogenesis while the remainder underwent limited spermatogenesis. A number of explanations may account for the levels of phenotypic penetrance and expressivity observed. First, the ablation performed may not eliminate the full set of somatic cells that participate in a given germline process. For instance, ablation of all somatic gonad cells at the L2/L3 molt, rather than just the SS cells, raises the percentage of arms lacking gametes from 43 to 92%. Additionally, direct ablation of all four proximal sheath cells in L4, rather than just elimination of two of the four by 1 SS cell ablation at the L2/L3 molt, raises the percentage of arms with the Emo phenotype from 44 to 95%. Second, cells next to those ablated appear to have some ability to compensate for their neighbor's absence. While somatic gonad lineage alterations do not occur to replace the ablated cells, we have observed sheath cells extending their area of coverage around the gonad arm into the regions that would have been occupied by the missing cells. This compensation may preserve functionality of the myoepithelium during ovulation and prevent the Emo phenotype in some cases. Third, the time at which the ablation was performed may affect the penetrance and expressivity of the phenotypes observed. For example, if the somatic gonad is signaling to promote the male germ cell fate from L1–L3, earlier ablation of somatic cells might increase the penetrance of feminization. Fourth, failure to kill the targeted cells by ablation may account for a small percentage of the incomplete penetrance. For instance, when only ablation samples verified by cell count upon dissection are considered, the penetrance of the Emo phenotype following 1 SS cell ablation rises slightly (from 44 to 51%). Ablations were verified whenever possible (see notes to tables) and are clearly not the major cause of incomplete penetrance. Fifth, in cases where soma to germline signaling is occurring, the cellular debris remaining after the death of the somatic cells by ablation

might still signal the germ line and thus account for some of the incomplete penetrance (Sulston and White, 1980). Sixth, some germline processes may have redundant controls and rely only partially on somatic cells. In these cases, even full elimination of all the somatic cells involved would not generate complete penetrance. Whatever the underlying cause(s), the incomplete penetrance of the somatic gonad ablation-induced germline phenotypes does not affect the conclusion that somatic cells likely play an important role in the above-described germline events.

The Proximal Sheath and Distal Spermatheca Function in Ovulation and Prevent the Accumulation of Endomitotic Oocytes in the Gonad Arm

During ovulation, the mature oocyte is forced out of the gonad arm by contractions of the proximal somatic sheath which pull the dilating distal spermatheca over the oocyte. Ablation of 1 SS cell, or direct ablation of either proximal sheath or distal spermathecal cells, disrupts ovulation. Oocytes mature but remain in the gonad arm because either (1) sheath contractions are insufficient for exit or (2) lack of a functional distal spermatheca allows ovulating oocytes to reflux back into the arm. While the remaining sheath cells following ablation expand their territories of coverage to make up for the missing cells, they are not capable of generating the same rate or intensity of contraction seen when a complete complement of sheath cells is present. Following unsuccessful ovulation, the mature oocytes remain in the arm and cycle endomitotically to become polyploid, a sterile phenotype referred to as Emo for endomitotic oocytes in the gonad arm (Iwasaki *et al.*, 1996). Following these ablations, gonads also show evidence of oocytes being torn during defective ovulation.

We considered a number of hypotheses for the origin of the Emo phenotype following SS lineage ablation before concluding that defective ovulation was the cause. For instance, elimination of somatic cells might allow immature oocytes to exit diakinesis and reenter the cell cycle or result in inappropriate activation of the oocyte by spermatids in the gonad arm. However, time-lapse Nomarski microscopy indicates that the first visible defects occur at the time of ovulation; oocytes develop and mature normally in order from distal to proximal as in wild type but fail in ovulation. Following 1 SS cell ablation in females, the Emo phenotype is observed, but with a delay. This delay is expected if the defect lies in ovulation following normal maturation, since feminization delays the onset of oocyte maturation (Iwasaki *et al.*, 1996). Endomitosis cannot result from an indirect effect of the somatic cell ablation on sperm, since the phenotype still arises in females where no sperm are present.

Function of the Sheath and Spermatheca in Ovulation

Like ablations which eliminate sheath cells, mutations which disrupt the sheath's contractile function cause defective ovulation and the Emo phenotype. The *unc-54(e190)* mutation, which eliminates myosin B, shows defective ovulation and the Emo phenotype at low penetrance. Interestingly, the mutation *mup-2(e2346ts)* results in fully penetrant sterility at 25°C with the Emo phenotype (Myers *et al.*, 1996). *mup-2* encodes a *C. elegans* troponin T, a protein known to be involved in regulation of muscle contraction. At 25°C, the sheath of *mup-2(e2346)* animals has no contractile activity and ovulation does not occur. Therefore, disruption of two components of the myofilament system within the sheath confirms the role of these cells in ovulation and further establishes a link between defective ovulation and the appearance of endomitotic oocytes in the gonad arm.

The requirement of the sheath and spermathecal cells for normal ovulation (i.e., preventing the Emo phenotype) is also indicated by mutations in genes required for specification or differentiation of these somatic cells. Development of oocytes in a male soma where sheath cells are lacking and ovulation is impossible generates an Emo phenotype (*fog-1* and *fog-3* XO). *shv-1(oz128),* which is missing the descendants of 1 SS cell (R. Francis, M. T. Le, and T. Schedl, unpublished results), also has endomitotic oocytes in the gonad arm. Mutations in *ceh-18* (Greenstein *et al.*, 1994), a gene encoding a sheath-expressed transcription factor, cause defective ovulation and the Emo phenotype. Since *ceh-18(mg57)* has other germline phenotypes similar to those found following sheath lineage cell ablation (i.e., defective germline proliferation and pachytene exit), it appears likely that CEH-18 is necessary for proper specification, differentiation, or general function of the sheath.

The oocyte itself also plays a role in the ovulation process. The sterile mutant *emo-1(oz1)* (Iwasaki *et al.*, 1996) displays the Emo phenotype and is defective in ovulation. Mosaic analysis demonstrates that a wild-type copy of the gene is needed in the germ line for fertility. *emo-1* encodes a homolog of Sec61 γ, a protein needed for ER translocation. We have proposed that defective ovulation in *emo-1(oz1)* results from a failure of the oocyte to signal the sheath and/or spermatheca at ovulation. Additional *emo* mutants may identify genes which act in either the germ line or soma during ovulation.

Sheath and Spermathecal Lineage Cells Aid in Germline Proliferation

The *C. elegans* gonad produces a steady supply of gametes by maintaining a mitotic germline stem cell population in the distal germ line. The DTC–GLP-1 signaling pathway promotes germline proliferation; the LAG-2 ligand, expressed in the DTC, signals the GLP-1 receptor, expressed in the germ line (see Introduction). The reduced germ cell number following elimination of both sheath/spermathecal precursors at the L2/L3 molt indicates that germline proliferation depends on these somatic cells as well.

Evidence indicates that the effect of sheath and spermathecal lineage cells on germ cell proliferation is independent of DTC-GLP-1 signaling. First, the role of the SS lineage

cells in promoting proliferation is distinct from that of the DTC. Following DTC ablation, the distal stem cell population is eliminated, whereas following 2 SS cell ablation, the stem cell population is maintained, although proliferation is reduced. The SS lineage cells, therefore, aid in proliferation, but unlike the DTC, they are neither necessary nor sufficient for proliferation. Second, in the mutant *glp-1(oz112gf),* where the GLP-1 receptor is constitutively active (Berry *et al.,* 1997), 2 SS cell ablation can still decrease germline proliferation in the gonad arm relative to a control arm where no cells were ablated. Third, the GLP-1 ligand LAG-2 is not detected in cells of the sheath and spermathecal lineage (D. L. Gao, S. T. Henderson, and J. Kimble, personal communication). The SS cells or their descendants may be providing an additional specific molecular signal to the germ line to directly stimulate germ cell proliferation. Such a pathway could act synergistically with the DTC–GLP-1 signaling pathway. It is also plausible that the SS cell lineage is providing nutritional support to the germ cells by transporting metabolites or macromolecules from the pseudocoelom into the gonad. Loss of this transport following SS cell lineage ablation would reduce nutrient availability and indirectly limit mitotic proliferation. Germline dependence on the soma for nutritional support is observed in mammals (Buccione *et al.,* 1987; Jegou, 1992).

It is possible that cells of the sheath and spermathecal lineages are involved in signaling for germline proliferation before distal restriction of the mitotic zone is completed. From L1 until at least late L2, proliferation occurs throughout the germline. During L3, a polarity is established with proliferation restricted to the distal region of each arm. By adulthood, germ line proliferation occurs only close to extended processes of the DTC where the level of membrane-associated GLP-1 protein is high (Crittenden *et al.,* 1994; Fitzgerald and Greenwald, 1995; D. L. Gao and J. Kimble, personal communication). The SS cells in late L2, and their descendants in L3 and early L4, are in close proximity to mitotic germ cells. In animals where no cells have been ablated, germ cell number increases greatly during L3 and L4, from ~20 per arm at the L2/L3 molt to over 500 by the L4/A molt. Reduction of proliferation during this period by the loss of the SS lineage cells may result in a smaller germ line which in adulthood cannot compensate for the proliferation missed in the larva. Alternatively, if sheath and spermathecal cell signaling does promote mitotic proliferation in the adult, the effect would have to be at a distance; germ cells near even the most distal sheath pair have a nuclear morphology indicative of meiotic prophase. (The nuclei of the most distal sheath cells are >25 μm from the mitotic zone in young adults.)

Sheath and Spermathecal Lineage Cells Promote Exit of Germ Cells from Pachytene and/or Promote Gametogenesis

C. elegans germ cells exit the pachytene stage of meiotic prophase and differentiate proximally. The extent to which the many steps of meiotic prophase progression and differentiation are germ cell autonomous versus somatically regulated is not yet defined. Hermaphrodite gonad arms following 2 SS cell ablation are sterile and capable of only limited gametogenesis, with many germ cells remaining in pachytene. The cells may be blocked in exit from pachytene or blocked in gametogenesis, or the two processes may be linked. The retention of germ cells in pachytene is not a consequence of the smaller size of the germ line following 2 SS ablation since ablation of germ cells at the L2/L3 molt can also reduce germline size without effecting pachytene exit or gametogenesis. Following ablation of distal sheath cells in L4, the zone of pachytene germ cells extends proximally beyond its usual boundary, indicating that the spatial position of pachytene exit may be altered. These results suggest that the sheath cells, and perhaps the spermathecal cells as well, may provide a signal to germ cells to exit the pachytene stage of meiotic prophase and/or undergo gametogenesis. *C. elegans* mutants in RAS and the MAP kinase pathway genes result in sterility with germ cells blocked in pachytene (Church *et al.,* 1995). The molecules which serve as the ligand and receptor for this pathway are not known. Could cells of the sheath and spermathecal lineages be providing an extracellular signal to activate this pathway in the germ line? Our ablation findings are consistent with this hypothesis. The somatic cells involved in signaling may also include the AC and the DU and VU cells and their descendants as well as the SS cells, since ablation of all somatic blast cells reduces gamete production more effectively than 2 SS cell ablation alone. Alternatively, the somatic cells may be providing nutritional support to the germ cells necessary for the high metabolic demands of gametogenesis.

The roles we have defined for the SS cell lineages in mitotic proliferation and pachytene exit/gametogenesis in hermaphrodites likely apply to the non-DTC somatic lineages of the *C. elegans* male as well. While male gonads do not generate sheath or spermathecal cells, they have similar blast cells which generate the vas deferens and seminal vesicle (Kimble and Hirsh, 1979). L1 ablation of all somatic cells except the DTC's in a male with a feminized germ line results in a gonad with reduced proliferation and severely limited gametogenesis (E. Lambie, personal communication).

Sheath and Spermathecal Lineage Cells May Promote the Male Fate in Hermaphrodite Germline Sex Determination

Germline and somatic sex determination in *C. elegans* proceed by similar genetic pathways (Hodgkin, 1990; Villeneuve and Meyer, 1990; Clifford *et al.,* 1994). Briefly, somatic sex is determined by the X chromosome to autosome ratio. A negative regulatory cascade of at least 12 genes interprets the ratio and communicates the determined sex to cells for proper development. The same basic negative regulatory cascade acts in the germ line with two exceptions. First, in hermaphrodites (which are somatically female), a brief period of spermatogenesis is allowed in L4 independent of

the X:A ratio. Second, additional genes act in germline sex determination which have no role in somatic sex determination (i.e., the *fog* and *mog* genes). The finding that ablation of 1 SS cell (or a DU cell) can feminize the germ line suggests that germline sex determination may have a nonautonomous component and thus depend upon the surrounding somatic cells. Surprisingly, the female somatic gonad would appear to signal the germ line to promote the male fate.

A cell-nonautonomous step is known to occur in XO male germline and somatic sex determination; the *her-1* gene encodes a putative secreted protein (Perry *et al.*, 1993) and has been demonstrated by mosaic analysis to function nonautonomously (Hunter and Wood, 1992). The HER-1 signal is likely received by the putative transmembrane protein TRA-2 (Okkema and Kimble, 1991; Kuwabara *et al.*, 1992; Kuwabara and Kimble, 1995). Genetic analysis places *tra-2* directly downstream of *her-1* in the sex determination pathway (Doniach, 1986; Kuwabara, 1996). HER-1 does not act in hermaphrodite germline sex determination; the *her-1* transcript that promotes male development is not expressed in XX hermaphrodites (Trent *et al.*, 1991; Perry *et al.*, 1993), and *her-1* null mutations have no phenotype in XX hermaphrodites (Hodgkin, 1980). However, ectopic production of HER-1 in the hermaphrodite can result in male germline development (Perry *et al.*, 1993), indicating that ligand-dependent TRA-2 activity can affect germline sex in the hermaphrodite. Thus, it is possible that ligand-dependent TRA-2 activity may control sex determination in wild-type hermaphrodites.

Currently, no nonautonomous factor has been demonstrated in *C. elegans* hermaphrodite germline sex determination, but the ablation results suggest that such a factor may exist. At least one gene, *fog-2* (Schedl and Kimble, 1988), may act at a position in the germline sex determination cascade similar to that of *her-1* (i.e., upstream of *tra-2*). Importantly, the *fog-2* phenotype is hermaphrodite specific (XX or XO), as would be predicted for a signal from the female somatic gonad. However, mutants in *fog-2* are capable of suppressing the *fem-3(q20gf)* Mog phenotype while 1 SS cell ablation cannot. Ultimately, demonstration of a somatic role in hermaphroditic germline sex determination will require the identification and characterization of a sex determination gene(s) that functions in the hermaphrodite somatic gonad.

ACKNOWLEDGMENTS

We thank Ross Francis, Kouichi Iwasaki, Mai Thao Le, Beth Bucher, David Greenstein, and Carol Myers for helpful discussions regarding the Emo phenotype. We appreciate Beth Bucher and David Greenstein providing strains before publication. UNC-87 antibody was generously provided by Sue Goetinck and Bob Waterston. We owe a debt to Jim Waddle for establishment of the departmental imaging center. Strains, reagents, experimental protocols, and productive suggestions were provided by Laura Wilson Berry, Bob Clifford, Ross Francis, Jonathan Hodgkin, Pam Hoppe, Allan Jones, Judith Kimble, Patty Kuwabara, Jeff Lichtman, Anna Newman, Mike Nonet, Larry Schriefer, Paresh Shrimankar, Bob Waterston, Shelly Weiss, Beth Westlund, Ben Williams, and John White. We thank Iva Greenwald, Pam Hoppe, and Jane Hubbard for comments on the manuscript. This research was supported by National Science Foundation Grant 9506220 to T.S. T.D. was supported by the National Science Foundation summer undergraduate research program in developmental biology (BIR-9531558); B.B. received support from a Howard Hughes Medical Institute Grant to the Young Scientist Program for high school student research at Washington University. Some strains used in this study were provided by the *Caenorhabditis* Genetics Center, which is supported by the National Institutes of Health's National Center for Research Resources.

REFERENCES

Abi-Rached, M., and Brun, J. L. (1975). Etude ultrastructurale des relations entre ovocytes et rachis au cours de l'ovogenese du nematode *C. elegans. Nematologica* **21,** 151–162.

Albertson, D. G. (1984). Formation of the first cleavage spindle in nematode embryos. *Dev. Biol.* **101,** 61–72.

Anderson, K. V., and Nusslein-Volhard, C. (1984). Information for the dorsal–ventral pattern of the *Drosophila* embryo is stored as maternal mRNA. *Nature* **311,** 223–227.

Austin, J., and Kimble, J. (1987). *glp-1* is required in the germ line for regulation of the decision between mitosis and meiosis in *C. elegans. Cell* **51,** 589–599.

Austin, J., and Kimble, J. (1989). Transcript analysis of *glp-1* and *lin-12,* homologous genes required for cell interactions during development of *Caenorhabditis elegans. Cell* **58,** 565–571.

Avery, L., and Horvitz, H. (1987). A cell that dies during wild-type *C. elegans* development can function as a neuron in a *ced-3* mutant. *Cell* **51,** 1071–1078.

Bargmann, C. I., and Avery, L. (1995). Laser killing of cells in *Caenorhabditis elegans. In* "Methods in Cell Biology" (H. F. Epstein and D. C. Shakes, Eds.), Vol. 48. Academic Press, San Diego.

Barton, M. K., and Kimble, J. (1990). *fog-1,* a regulatory gene required for specification of spermatogenesis in the germ line of *Caenorhabditis elegans. Genetics* **125,** 29–39.

Barton, M. K., Schedl, T. B., and Kimble, J. (1987). Gain-of-function mutations of *fem-3,* a sex-determination gene in *Caenorhabditis elegans. Genetics* **115,** 107–119.

Beitel, G. J., Clark, S. G., and Horvitz, H. R. (1990). *Caenorhabditis elegans* ras gene *let-60* acts as a switch in the pathway of vulval induction. *Nature* **348,** 503–509.

Berry, L. W., Westlund, B., and Schedl, T. (1997). Germline tumor formation caused by activation of *glp-1,* a *C. elegans* member of the Notch family of receptors. *Development,* in press.

Bownes, M. (1994). Interactions between germ cells and somatic cells in *Drosophila melanogaster. Semin. Dev. Biol.* **5,** 31–42.

Brenner, S. (1974). The genetics of *Caenorhabditis elegans. Genetics* **77,** 71–94.

Buccione, R., Cecconi, S., Tatone, C., Mangia, F., and Colonna, R. (1987). Follicle cell regulation of mammalian oocyte growth. *J. Exp. Zool.* **242,** 351–354.

Buccione, R., Schroeder, A. C., and Eppig, J. J. (1990). Interactions between somatic cells and germ cells through mammalian oogenesis. *Biol. Reprod.* **43,** 543–547.

Chasan, R., and Anderson, K. (1989). The role of *easter,* an apparent serine protease, in organizing the dorsal–ventral pattern of the *Drosophila* embryo. *Cell* **56,** 391–400.

Church, D. L., Guan, K. L., and Lambie, E. J. (1995). Three genes of the MAP kinase cascade, *mek-2, mpk-1/sur-1,* and *let-60 ras,* are required for meiotic cell cycle progression in *Caenorhabditis elegans. Development* **121,** 2525–2535.

Clifford, R., Francis, R., and Schedl, T. (1994). Somatic control of germ cell development in *Caenorhabditis elegans. Semin. Dev. Biol.* **5,** 21–30.

Crittenden, S. L., Troemel, E. R., Evans, T. C., and Kimble, J. (1994). GLP-1 is localized to the mitotic region of the *C. elegans* germ line. *Development* **120,** 2901–2911.

Diaz-Infante, A., Jr., Wright, B. S., and Wallach, E. E. (1975). Influence of estrogen and progesterone treatment on ovarian contractility in the monkey. *Fertil. Steril.* **26,** 101–110.

Dibb, N. J., Brown, D. M., Karn, J., Moerman, D. G., Bolten, S. L., and Waterston, R. H. (1985). Sequence analysis of mutations that affect the synthesis, assembly and enzymatic activity of the *unc-54* myosin heavy chain of *Caenorhabditis elegans. J. Mol. Biol.* **183,** 543–551.

Dolci, S., Williams, D. E., Ernst, M. K., Resnick, J. L., Brannan, C. I., Lock, L. F., Lyman, S. D., Boswell, H. S., and Donovan, P. J. (1991). Requirement for mast cell growth factor for primordial germ cell survival in culture. *Nature* **352,** 809–811.

Doniach, T. (1986). Activity of the sex-determining gene *tra-2* is modulated to allow spermatogenesis in the *C. elegans* hermaphrodite. *Genetics* **114,** 53–76.

Doniach, T., and Hodgkin, J. (1984). A sex-determining gene, *fem-1,* required for both male and hermaphrodite development in *Caenorhabditis elegans. Dev. Biol.* **106,** 223–235.

Edgar, L. G., and Hirsh, D. (1985). Use of a psoralen-induced phenocopy to study genes controlling spermatogenesis in *Caenorhabditis elegans. Dev. Biol.* **111,** 108–118.

Ellis, H. M., and Horvitz, H. R. (1986). Genetic control of programmed cell death in the nematode *C. elegans. Cell* **44,** 817–829.

Ellis, R. E., and Kimble, J. (1995). The *fog-3* gene and regulation of cell fate in the germ line of *Caenorhabditis elegans. Genetics* **139,** 561–577.

Ferguson, E. L., and Horvitz, H. R. (1985). Identification and characterization of 22 genes that affect the vulval cell lineages of the nematode *Caenorhabditis elegans. Genetics* **110,** 17–72.

Fitzgerald, K., and Greenwald, I. (1995). Interchangeability of *Caenorhabditis elegans* DSL proteins and intrinsic signalling activity of their extracellular domains *in vivo. Development* **121,** 4275–4282.

Fleischman, R. A. (1993). From white spots to stem cells: The role of the Kit receptor in mammalian development. *Trends Genet.* **9,** 285–290.

Fodor, A., Riddle, D. L., Nelson, F. K., and Golden, J. W. (1983). Comparison of a new wild-type *Caenorhabditis briggsae* with laboratory strains of *C. briggsae* and *C. elegans. Nematologica* **29,** 203–217.

Francis, R., Barton, M. K., Kimble, J., and Schedl, T. (1995). *gld-1,* a tumor suppressor gene required for oocyte development in *Caenorhabditis elegans. Genetics* **139,** 607–630.

Gibert, M. A., Starck, J., and Beguet, B. (1984). Role of the gonad cytoplasmic core during oogenesis of the nematode *Caenorhabditis elegans. Biol. Cell* **50,** 77–85.

Godin, I., Deed, R., Cooke, J., Zsebo, K., Dexter, M., and Wylie, C. C. (1991). Effects of the steel gene product on mouse primordial germ cells in culture. *Nature* **352,** 807–809.

Goetinck, S., and Waterston, R. H. (1994). The *Caenorhabditis elegans* muscle-affecting gene *unc-87* encodes a novel thin filament-associated protein. *J. Cell Biol.* **127,** 79–93.

Greenstein, D., Hird, S., Plasterk, R. A., Adachi, Y., Kohara, Y., Wang, B., Finney, M., and Ruvkun, G. (1994). Targeted mutations in the *C. elegans* POU-homeobox gene *ceh-18* cause defects in oocyte cell cycle arrest, gonad migration, and epidermal differentiation. *Genes Dev.* **8,** 1935–1948.

Han, M., and Sternberg, P. W. (1990). *let-60,* a gene that specifies cell fates during *C. elegans* vulva induction, encodes a *ras* protein. *Cell* **63,** 921–931.

Hedgecock, E. M., and Herman, R. K. (1995). The *ncl-1* gene and genetic mosaics of *Caenorhabditis elegans. Genetics* **141,** 989–1006.

Henderson, S. T., Gao, D., Lambie, E. J., and Kimble, J. (1994). *lag-2* may encode a signaling ligand for the GLP-1 and LIN-12 receptors of *C. elegans. Development* **120,** 2913–2924.

Hirsh, D., Oppenheim, D., and Klass, M. (1976). Development of the reproductive system of *Caenorhabditis elegans. Dev. Biol.* **49,** 200–219.

Hodgkin, J. (1980). More sex-determination mutants of *Caenorhabditis elegans. Genetics* **96,** 649–664.

Hodgkin, J. (1986). Sex determination in the nematode *Caenorhabditis elegans:* Analysis of *tra-3* suppressors and characterization of the *fem* genes. *Genetics* **114,** 15–52.

Hodgkin, J. (1990). Sex determination compared in *Drosophila* and *Caenorhabditis elegans. Nature* **344,** 721–728.

Hodgkin, J. A., and Brenner, S. (1977). Mutations causing transformation of sexual phenotype in the nematode *Caenorhabditis elegans. Genetics* **86,** 275–287.

Hunter, C. P., and Wood, W. B. (1992). Evidence from mosaic analysis of the masculinizing gene *her-1* for cell interactions in *C. elegans* sex determination. *Nature* **355,** 551–555.

Iwasaki, K., McCarter, J., Francis, R., and Schedl, T. (1996). *emo-1,* a *Caenorhabditis elegans* Sec61p gamma homologue, is required for oocyte development and ovulation. *J. Cell Biol.* **134,** 699–714.

Jegou, B. (1992). The Sertoli cell *in vivo* and *in vitro. Cell Biol. Toxicol.* **8,** 49–54.

Kimble, J. (1981). Alterations in cell lineage following laser ablation of cells in the somatic gonad of *Caenorhabditis elegans. Dev. Biol.* **87,** 286–300.

Kimble, J., Edgar, L., and Hirsh, D. (1984). Specification of male development in *Caenorhabditis elegans:* The *fem* genes. *Dev. Biol.* **105,** 234–239.

Kimble, J., and Hirsh, D. (1979). Postembryonic cell lineages of the hermaphrodite and male gonads in *Caenorhabditis elegans. Dev. Biol.* **70,** 396–417.

Kimble, J., and Ward, S. (1988). Germline development and fertilization. *In* "The Nematode *Caenorhabditis elegans*" (W. B. Wood, Ed.), pp. 191–213. Cold Spring Harbor Laboratory Press, Cold Spring Harbor, NY.

Kimble, J. E., and White, J. G. (1981). On the control of germ cell development in *Caenorhabditis elegans. Dev. Biol.* **81,** 208–219.

Kirby, C., Kusch, M., and Kemphues, K. (1990). Mutations in the *par* genes of *Caenorhabditis elegans* affect cytoplasmic reorganization during the first cell cycle. *Dev. Biol.* **142,** 203–215.

Klass, M., Wolf, N., and Hirsh, D. (1976). Development of the male reproductive system and sexual transformation of the nematode *Caenorhabditis elegans. Dev. Biol.* **52,** 1–18.

Kornfeld, K., Guan, K.-L., and Horvitz, H. R. (1995). The *Caenorhabditis elegans* gene *mek-2* is required for vulval induction and encodes a protein similar to the protein kinase MEK. *Genes Dev.* **9,** 756–768.

Kuwabara, P. E. (1996). A novel regulatory mutation in the *C. elegans* sex determination gene *tra-2* defines a candidate ligand/receptor interaction site. *Development* **122,** 2089–2098.

Kuwabara, P. E., and Kimble, J. (1995). A predicted membrane protein, TRA-2A, directs hermaphrodite development in *Caenorhabditis elegans. Development* **121,** 2995–3004.

Kuwabara, P. E., Okkema, P. G., and Kimble, J. (1992). *tra-2* encodes a membrane protein and may mediate cell communication in the *Caenorhabditis elegans* sex determination pathway. *Mol. Biol. Cell* **3,** 461–473.

Lackner, M. R., Kornfeld, K., Miller, L. M., Horvitz, H. R., and Kim, S. K. (1994). A MAP kinase homolog, *mpk-1,* is involved in ras-mediated induction of vulval cell fates in *Caenorhabditis elegans. Genes Dev.* **8,** 160–173.

Lambie, E. J., and Kimble, J. (1991). Two homologous regulatory genes, *lin-12* and *glp-1,* have overlapping functions. *Development* **112,** 231–240.

MacLeod, A. R., Waterston, R. H., and Brenner, S. (1977). An internal deletion mutant of a myosin heavy chain in *Caenorhabditis elegans. Proc. Natl. Acad. Sci. USA* **74,** 5336–5340.

McLaren, A. (1991). Development of the mammalian gonad: The fate of the supporting cell lineage. *Bioessays* **13,** 151–156.

Miller, D. M., Stockdale, F. E., and Karn, J. (1986). Immunological identification of the genes encoding the four myosin heavy chain isoforms of *Caenorhabditis elegans. Proc. Natl. Acad. Sci. USA* **83,** 2305–2309.

Myers, C. D., Goh, P. Y., Allen, T. S., Bucher, E. A., and Bogaert, T. (1996). Developmental genetic analysis of troponin T mutations in striated and non-striated muscle cells of *C. elegans. J. Cell Biol.* **132,** 1061–1077.

Nelson, G. A., Lew, K. K., and Ward, S. (1978). *Intersex,* a temperature-sensitive mutant of the nematode *Caenorhabditis elegans. Dev. Biol.* **66,** 386–409.

Neuman-Silberberg, F. S., and Schupbach, T. (1993). The *Drosophila* dorsoventral patterning gene *gurken* produces a dorsally localized RNA and encodes a TGF alpha-like protein. *Cell* **75,** 165–174.

Newman, A. P., White, J. G., and Sternberg, P. W. (1995). The *Caenorhabditis elegans lin-12* gene mediates induction of ventral uterine specialization by the anchor cell. *Development* **121,** 263–271.

Norman, G. R., and Streiner, D. L. (1994). ''Biostatistics, the Bare Essentials.'' Mosby, St. Louis.

Nothinger, R., Jonglez, M., Leuthold, M., Meier-Gerschwiler, P., and Weber, T. (1989). Sex determination in the germ line of *Drosophila* depends on genetic signals and inductive somatic factors. *Development* **107,** 505–518.

Okkema, P. G., Harrison, S. W., Plunger, V., Aryana, A., and Fire, A. (1993). Sequence requirements for myosin gene expression and regulation in *Caenorhabditis elegans. Genetics* **135,** 385–404.

Okkema, P. G., and Kimble, J. (1991). Molecular analysis of *tra-2,* a sex determining gene in *Caenorhabditis elegans. EMBO J.* **10,** 171–176.

Perry, M. D., Li, W., Trent, C., Robertson, B., Fire, A., Hageman, J., and Wood, W. B. (1993). Molecular characterization of the *her-1* gene suggests a direct role in cell signaling during *Caenorhabditis elegans* sex determination. *Genes Dev.* **7,** 216–228.

Priess, J. R., Schnabel, H., and Schnabel, R. (1987). The *glp-1* locus and cellular interactions in early *C. elegans* embryos. *Cell* **51,** 601–611.

Ray, R. P., and Schupbach, T. (1996). Intercellular signaling and the polarization of body axes during *Drosophila* oogenesis. *Genes Dev.* **10,** 1711–1723.

Roth, S., Neuman-Silberberg, F. S., Barcelo, G., and Schupbach, T. (1995). *cornichon* and the EGF receptor signaling process are necessary for both anterior–posterior and dorsal–ventral pattern formation in *Drosophila. Cell* **81,** 967–978.

Ruohola, H., Bremer, K. A., Baker, D., Swedlow, J. R., Jan, L. Y., and Jan, Y. N. (1991). Role of neurogenic genes in establishment of follicle cell fate and oocyte polarity during oogenesis in *Drosophila. Cell* **63,** 433–449.

Schedl, T., and Kimble, J. (1988). *fog-2,* a germ-line-specific sex determination gene required for hermaphrodite spermatogenesis in *Caenorhabditis elegans. Genetics* **119,** 43–61.

Schüpbach, T. (1987). Germ line and soma cooperate during oogenesis to establish the dorsoventral pattern of egg shell and embryo in *Drosophila melanogaster. Cell* **49,** 699–707.

Seydoux, G., Schedl, T., and Greenwald, I. (1990). Cell–cell interactions prevent a potential inductive interaction between soma and germline in *Caenorhabditis elegans. Cell* **61,** 939–951.

St. Johnston, D. (1994). RNA localization. Getting to the top. *Curr. Biol.* **4,** 54–56.

Stein, D., Roth, S., Vogelsang, E., and Nusslein-Volhard, C. (1991). An activity present in the previtelline space of the *Drosophila* egg determines the dorsoventral axis of the embryo. *Cell* **65,** 725–735.

Steinmann-Zwicky, M. (1992). Sex determination of *Drosophila* germ cells. *Semin. Dev. Biol.* **3,** 341–347.

Steinmann-Zwicky, M., Schmid, H., and Nothiger, R. (1989). Cell-autonomous and inductive signals can determine the sex of the germ line of *Drosophila* by regulating the gene *Sxl. Cell* **57,** 157–166.

Strome, S. (1986). Fluorescence visualization of the distribution of microfilaments in gonads and early embryos of the nematode *C. elegans. J. Cell Biol.* **103,** 2241–2252.

Sulston, J., and Hodgkin, J. (1988). Methods. *In* ''The Nematode *Caenorhabditis elegans*'' (W. B. Wood, Ed.), pp. 587–606. Cold Spring Harbor Laboratory Press, Cold Spring Harbor, NY.

Sulston, J. E., and White, J. G. (1980). Regulation and cell autonomy during postembryonic development of *Caenorhabditis elegans. Dev. Biol.* **78,** 577–597.

Sundaram, M., Yochem, J., and Han, M. (1996). A Ras-mediated signal transduction pathway is involved in the control of sex myoblast migration in *Caenorhabditis elegans. Development* **122,** 2823–2833.

Tax, F. E., Yeargers, J. J., and Thomas, J. H. (1994). Sequence of *C. elegans lag-2* reveals a cell-signalling domain shared with *Delta* and *Serrate* of *Drosophila. Nature* **368,** 150–154.

Trent, C., Purnell, B., Gavinski, S., Hageman, J., Chamblin, C., and Wood, W. (1991). Sex-specific transcriptional regulation of the *C. elegans* sex-determining gene *her-1. Mech. Dev.* **34,** 43–56.

Villeneuve, A. M., and Meyer, B. J. (1990). The regulatory hierarchy controlling sex determination and dosage compensation in *Caenorhabditis elegans. In* ''Advances in Genetics'' (J. G. Scandalios and T. R. F. Wright, Eds.), pp. 117–188. Academic Press, New York.

Ward, S., and Carrel, J. S. (1979). Fertilization and sperm competition in the nematode *Caenorhabditis elegans. Dev. Biol.* **73,** 304–321.

Waterston, R. H., Thomson, J. N., and Brenner, S. (1980). Mutants with altered muscle structure of *Caenorhabditis elegans. Dev. Biol.* **77,** 271–302.

White, J. G. (1988). The anatomy. *In* ''The Nematode *Caenorhab-*

ditis elegans'' (W. B. Wood, Ed.). Cold Spring Harbor Laboratory Press, Cold Spring Harbor, NY.

Wickramasinghe, D., and Albertini, D. F. (1993). Cell cycle control during mammalian oogenesis. *Curr. Top. Dev. Biol.* **28,** 125–153.

Wu, Y., and Han, M. (1994). Suppression of activated LET-60 Ras protein defines a role of *Caenorhabditis elegans* SUR-1 MAP kinase in vulval differentiation. *Genes Dev.* **8,** 147–159.

Wu, Y., Han, M., and Guan, K.-L. (1995). MEK-2, a *Caenorhabditis elegans* MAP kinase kinase, functions in Ras-mediated vulval induction and other developmental events. *Genes Dev.* **9,** 742–755.

Yochem, J., and Greenwald, I. (1989). *glp-1* and *lin-12,* genes implicated in distinct cell–cell interactions in *Caenorhabditis elegans,* encode similar transmembrane proteins. *Cell* **58,** 553–563.

Received for publication September 4, 1996
Accepted October 1, 1996